

STANDARD GLOBULAR CLUSTER GIANT BRANCHES IN THE $(M_I, (V-I)_0)$ PLANEG. S. DA COSTA^{a), b)}

Yale University Observatory, Box 6666, New Haven, Connecticut 06511

T. E. ARMANDROFF

Kitt Peak National Observatory, National Optical Astronomy Observatories, Box 26732, Tucson, Arizona 85726

Received 22 January 1990; revised 16 March 1990

ABSTRACT

Photometry has been obtained in the V, I (Cousins) system for a large number of giants in six Galactic globular clusters that cover a wide range of metal abundance. The data were derived from CCD observations on the 0.9 m telescope at CTIO over three successive seasons. Both internal checks, and external comparisons with globular cluster stars measured by conventional photoelectric photometry, suggest that the CCD photometry is accurately on the standard system, and that the cluster star colors and magnitudes have overall uncertainties of less than 0.02 mag. These data, together with a cluster distance scale, which we take as that derived from recent horizontal branch models, allow the construction of cluster giant branches in a $(M_I, (V-I)_0)$ color-magnitude diagram. This diagram is then used to derive metal abundance estimates, relative to the abundances assumed for the calibrating clusters, for the globular clusters Pal 12 and Eridanus from V, I photometry of their giants. The abundances derived are $[Fe/H] = -1.06 \pm 0.12$ and $[Fe/H] = -1.50 \pm 0.15$, respectively. Further, the photometry is used to set 3σ upper limits in the range 0.04–0.09 dex for any intrinsic heavy-element abundance dispersion in the six calibrating clusters. The observed giant branches are also compared with the predictions of theory. In particular, we give a calibration of the bolometric correction to I magnitudes as a function of $(V-I)_0$ color. With this calibration and our adopted distance scale, we compare the bolometric magnitude of the brightest giant in each cluster with theoretical calculations of the luminosity of the helium core flash, finding acceptable agreement. The agreement is significantly worse, however, if the globular cluster distance scale advocated by Sandage is used instead. Further, we point out that the “semiempirical” method used to generate the giant branch data included with the Revised Yale Isochrones is valid only for a particular choice of distance scale. On this scale, which is not that of the horizontal branch models, the observed and theoretical giant branches agree reasonably well, though the deviations in color at high luminosities remain substantial.

I. INTRODUCTION

The advent of CCD detectors has instigated a revolution in astronomy in which problems previously thought to be unassailable are now routinely attacked. This is particularly true in the field of stellar populations research, where, for example, color-magnitude ($c-m$) diagrams for Local Group and other nearby galaxies are becoming not only increasingly common but also more precise. This proliferation of new results will no doubt increase as the *Hubble Space Telescope* goes into operation.

For many of these types of problems, it is advantageous to utilize the larger color baseline offered by the CCD response through the use of bandpasses other than the traditional B and V of the Johnson system. However, the move away from $(V, B-V)$ $c-m$ diagrams is often hampered by the lack of suitable well-studied standard objects with which comparisons can be made. For example, in the pioneering $c-m$ diagram study of the giant branch in the M31 dE companion NGC 147 by Mould, Kristian, and Da Costa (1983) (hereafter referred to as MKD), the observations were carried out in the V, I (Cousins) system. The mean metal abundance, abundance dispersion, and distance of the galaxy were all

determined from these V, I data by comparing the NGC 147 photometry with that for giants in a small sample of globular clusters that covered a range in metal abundance. These standard cluster giant branches were defined by relatively small numbers of stars which, in fact, had not even been observed in the V, I (Cousins) system, but had instead been transformed from observations in the CMT_1, T_2 system [see Norris, Bessell, and Pickles (1985) for a discussion]. Nevertheless, these V, I cluster giant branches have been widely used (e.g., Richer, Crabtree, and Pritchett 1984; Heasley *et al.* 1988) because, with the exception of the photometry of Lloyd Evans (1983), there exists very little published V, I photometry for giants in “standard” galactic globular clusters. Even the Lloyd Evans (1983) photometry, however, is generally restricted only to brighter stars in the more metal-rich clusters.

To redress this situation, we present in this paper photometry on the V, I (Cousins) system for a large number of giants covering a wide range of absolute magnitude in six well-studied galactic globular clusters. These clusters have abundances that range from among the most metal-poor to that of the archetypal metal-rich cluster 47 Tuc. The photometry has been obtained with a CCD detector, and in Sec. II we describe the observation and reduction procedures. Comparison with available photoelectric photometry suggests that the CCD photometry is quite accurate, with the individual color and magnitude errors for the cluster stars being less than 0.02 mag.

The cluster photometry, together with an assumed distance scale, is then used in Sec. III to construct giant

^{a)} Visiting Astronomer, Cerro Tololo Inter-American Observatory, NOAO. NOAO is operated by AURA, Inc., under contract with the National Science Foundation.

^{b)} Present Address: Anglo-Australian Observatory, P.O. Box 296, Epping, NSW, 2121 Australia.

branches in the $(M_I, (V - I)_0)$ plane. The sensitivity of giant branch color to abundance is investigated and an abundance calibration, based on published abundances for the six standard clusters, is determined. This calibration is then used to set limits on the internal abundance dispersion in each of the six standard clusters and to determine abundance estimates for two halo globular clusters of current interest. These clusters are Pal 12, for which Stetson *et al.* (1989) have recently determined an age that is substantially younger than that of other halo clusters, and Eridanus, a cluster which previous abundance estimates (Da Costa 1985) have suggested is one of the most metal-rich clusters in the extreme outer halo of the Galaxy.

In Sec. IV the cluster giant branch results are compared with the predictions of theory. First, after determining bolometric corrections to the I magnitudes as a function of $(V - I)_0$ color, the absolute bolometric magnitude of the brightest giant in each cluster, for our adopted distance scale, is compared with theoretical predictions of the luminosity of the helium core flash. The agreement found is quite satisfactory indicating, *inter alia*, that the giant branch tip luminosity can be used as a distance indicator for old stellar populations. Second, we compare the observed giant branches with those from theory as contained in the Revised Yale Isochrones (Green, Demarque, and King 1987). This comparison is of interest since the theoretical giant branches are sometimes used to interpret observations when the abundance range of the empirical calibration is exceeded (e.g., Freedman 1989). The implications of the results of this comparison are discussed in some detail. Finally the major results are summarized in Sec. V.

II. PHOTOMETRY

a) Observations

The observations for this program were made with the CTIO 0.9 m telescope CCD camera over three successive observing seasons (November 1985, September 1986, and November 1987), with data being obtained on a total of eight photometric nights. The detector was always an RCA CCD, though two different chips (RCA4 and RCA5) were used in the different runs. Due to degradation of some of the filters, it was also not possible to use the same filter set for all three runs, though each set used corresponded to the "Mould" specifications [see, for example, Appendix VII in Schoening (1988)]. The scale at the detector of 0.495 "/pixel was a good match to the image profiles, which ranged from 1.1" (FWHM) on the best-seeing frames to 2.4" on the worst.

The fields observed in the six standard globular clusters [M15 (NGC 7078), NGC 6397, M2 (NGC 7089), NGC 6752, NGC 1851, and 47 Tuc (NGC 104)] were initially chosen because they contained one or more stars whose V and I magnitudes were required for other programs. These stars are generally relatively uncrowded and exposure times were set so that they were exposed to similar intensity levels as the standards. Actual integration times varied from a few seconds for the brightest giants in the nearby clusters NGC 6397, NGC 6752, and 47 Tuc, to 1–2 min for the fainter giants in the more distant clusters M15, M2, and NGC 1851.

Observations of the Pal 12 and Eridanus clusters were obtained in both the September 1986 and November 1987 runs, though for Eridanus the 1987 data (three 1200 s V and three 900 s I frames) are considerably superior to those obtained in 1986 (single 900 s V and 600 s I frames). For this

cluster the repeated exposure frames were combined using the codes available in IRAF into a single V, I frame pair prior to measurement.

b) Measurement and Reduction

On each photometric night, some 15–20 standards chosen from the lists of Landolt (1983) and Graham (1982) were observed, some more than once. The procedures used in acquiring, measuring, and reducing these standard star observations are fully described in Da Costa (1990) and need not be repeated here. It is sufficient to say that the transformations from the instrumental system to the standard system were always well behaved, with very small uncertainties in the transformation coefficients and typical rms residuals about the fits of 0.006 mag or less.

The stars on the globular cluster frames were measured in the same way as for the standard stars, i.e., via aperture photometry. However, with the exception of a small number of well-exposed uncrowded stars which were measured through a series of larger apertures in the same way as for the standards, the stars on the globular cluster frames were measured only through small apertures, typically 2.5–4 pixels (1.2"–2.0") in radius, to minimize both contamination from neighbors and photometric errors. The large-aperture measures on the uncrowded bright stars were used to determine the aperture corrections, i.e., the difference between the small-aperture magnitudes and the "total" or seeing-independent magnitude for the stars on each frame. There was always at least one such star on each frame and often more, in which case the individual aperture correction determinations were averaged. Because high accuracy rather than completeness was the goal, only those stars which were relatively uncrowded and which had sufficient photons for the small-aperture measures to have formal photon errors of 0.01 mag or less were actually measured on the individual globular cluster frames.

The resulting photometry is given in Tables I–VIII for 47 Tuc, NGC 1851, NGC 6752, M2, NGC 6397, M15, Pal 12, and Eridanus, respectively. Literature references for the cluster star identifications are given with the tables except for a small number of previously unidentified NGC 1851 stars, for which a chart is given in Fig. 1. Aside from the V magnitudes and $V - I$ colors on the Cousins (1976a,b) system, the tables also list the number of times a star was observed. In cases of multiple observations, the individual de-

TABLE I. 47 Tuc photometry.

Star ^a	V	$V - I$	N_{obs}
L3512	11.777	1.961	4
L5312	12.185	1.549	3
L5406	12.828	1.302	1
L5422	12.470	1.402	4
L5423	13.534	0.836	4
L5635	14.046	0.865	1
L5636	12.639	1.193	1
L5640	15.054	1.001	2
L5642	14.097	0.921	2
L5644	14.116	0.914	2
L5645	13.679	1.093	2
L6601	13.954	0.931	2
L6602	14.747	0.968	2
L6603	14.080	0.898	2
L6604	14.097	0.929	1

^aStar numbers from Lee (1977).

TABLE II. NGC 1851 photometry.

Star	V	$V-I$	N_{obs}	Star	V	$V-I$	N_{obs}
S107 ^a	14.515	1.210	2	S325	16.192	0.761	2
S109	14.854	1.153	1	S326	15.953	0.991	2
S112	13.832	1.426	2	S327	15.725	1.000	2
S126	14.360	1.288	1	S329	13.427	1.622	2
S129	14.453	1.228	1	S333	14.040	1.314	2
S136	14.891	1.172	1	S336	15.011	1.106	4
S137	14.854	1.064	1	S342	16.173	0.771	2
S151	13.817	1.392	2	S347	16.199	0.769	2
S164	14.402	1.237	2	S351	15.688	1.030	2
S173	15.854	0.999	2	S354	16.001	0.875	2
S175	16.261	1.006	1	S355	16.206	0.798	2
S176	15.588	1.012	2	S356	16.141	0.767	2
S183	15.427	0.972	2	S357	15.927	0.878	1
S262	13.374	1.567	1	S358	16.071	0.809	2
S279	13.992	1.320	2	S361	15.633	1.014	2
S293	15.247	1.070	1	S371	16.067	0.788	1
S294	13.440	1.580	2	S376	14.902	1.109	2
S297	15.464	1.058	2	DA1 ^b	14.531	1.159	4
S301	16.094	1.003	1	DA2	14.526	1.156	1
S306	15.670	1.009	2	DA3 ^c	13.110	0.602	2
S311	16.113	0.981	2	DA4	14.917	1.032	2
S315	16.042	0.835	1	DA6	13.294	1.815	1
S319	14.846	1.121	4	DA7	13.369	1.487	1
S320	14.931	0.878	4	DA11	15.001	1.140	1
S321	16.198	0.787	2	DA12	14.879	1.051	1
S324	15.934	0.854	2				

^a Star numbers from Stetson (1981).^b Star identifications given in Fig. 1.^c Star UV6 of Vidal and Freeman (1975), radial velocity nonmember (Seitzer 1989, private communication).

terminations were averaged without weighting, the sole exception being the Eridanus cluster, where the 1987 photometry was given three times the weight of that from the 1986 season.

The precision of the photometry has been investigated in a number of ways. First, since most of the cluster fields have been observed on more than one night, an error estimate can

TABLE III. NGC 6752 photometry.

Star	V	$V-I$	N_{obs}	Star	V	$V-I$	N_{obs}
CS3 ^a	11.505	1.316	2	A34	12.441	1.054	1
CL8 ^b	13.721	0.997	1	A35	12.171	1.102	1
CL10	13.641	1.016	1	A47	14.572	0.937	1
CL50	13.659	1.008	1	A48	13.003	1.091	1
CL64	13.995	0.991	1	A53	13.626	0.923	1
CL96	14.776	0.956	1	A54	13.819	0.819	1
CL97	14.666	0.964	1	A58	12.671	1.003	1
CL98	14.663	0.967	1	A59	10.887	1.607	2
CL100	14.563	-0.002	1	A61	11.595	1.264	2
CL101	14.970	1.083	1	A104	12.732	0.925	1
CL114	14.805	0.941	1	A105	12.262	1.163	1
A2 ^c	12.563	1.044	1	A109	13.284	1.021	1
A3	12.001	1.205	1	A130	13.708	0.998	2
A4	13.729	0.993	1	A140	12.794	1.087	1
A5	13.662	1.022	1	A141	13.556	1.009	2
A8	12.024	1.215	1	A142	14.112	0.934	1
A10	12.806	0.980	1	A146	13.645	0.986	1
A11	12.281	0.845	1	A153	13.662	0.980	1
A12	11.245	1.425	2	A156	13.922	0.978	1
A14	13.802	1.024	1	A158	14.072	0.945	1
A16	11.563	2.261	1	A159	13.070	1.077	1
A28	13.338	1.047	2	A160	12.008	1.220	1
A29	11.845	1.252	2	A161	13.683	1.025	1
A30	12.181	1.185	2	A183a ^d	13.065	1.054	1
A31	10.843	1.666	2	A246	14.571	0.961	1
A32	13.606	1.005	1	A336	12.355	1.126	1
A33	12.302	1.162	2				

^a Star number from Cannon and Stobie (1973).^b Star numbers from Cannon and Lee (unpublished).^c Star numbers from Alcaino (1972).^d This star lies 34" N and 2" W of star A33, just W of the fainter star A183.

be calculated from the repeat measurements. However, because in this situation the same stars have been used to determine the aperture corrections, the true errors will generally be underestimated. A more reliable error estimate results when fields which use different aperture correction stars partially overlap. This occurs for ten fields in four clusters, and for the 41 stars with at least two independent magnitudes and colors, the mean absolute value of the differences in V is 0.002 mag while the standard deviation of these differences is 0.011 mag. The corresponding values for the $V-I$ colors are 0.001 and 0.010 mag, respectively. These numbers are gratifyingly small.

The third means of investigating the precision of the data, which is the one that is most sensitive to deviations from the standard system, is a comparison of the CCD photometry with magnitudes and colors determined independently, generally by conventional photoelectric photometry. Considering first the $V-I$ colors, we show in Fig. 2 a comparison of the CCD $V-I$ colors with those determined by conventional photometry for stars in NGC 6397, NGC 6752, and 47 Tuc. The sources of the photoelectric photometry are Green (1987) and Lloyd Evans (1983). There is no indication of any systematic trend with color, and the mean difference, in the sense $(V-I)_{\text{CCD}} - (V-I)_{\text{PE}}$, is 0.006 mag. This offset is perhaps not unexpected since Cousins (1984) has shown that the standards of Landolt (1983), which calibrate the CCD photometry, are systematically too red by 0.012 ± 0.004 mag for $V-I > 1.0$. The photoelectric photometry, on the other hand, is calibrated directly with Cousins standards. Nevertheless, the standard deviation of the differences is only 0.016 mag, which, assuming equal errors in the photoelectric and CCD photometry, suggests that the CCD colors of these stars have 1σ uncertainties of approximately 0.011 mag.

Unlike the case of the $V-I$ colors, there exists a large amount of V -band photoelectric photometry for these clusters and so we consider a number of separate comparisons. First, in Fig. 3(a), we compare the CCD V magnitudes with the corresponding photoelectric values for stars in NGC 6397, NGC 6752, and 47 Tuc. The sources of the photoelectric photometry are Cannon (1974) for NGC 6397, Cannon and Stobie (1973) for NGC 6752, and Cannon (1974), Green (1987), and Lloyd Evans (1983) for 47 Tuc. As for the $V-I$ colors there are no systematic trends with magnitude (or color), indicating that the CCD observations are accurately on the standard system. The mean difference, again in the sense $V_{\text{CCD}} - V_{\text{PE}}$, is 0.004 mag while the standard deviation of the differences is 0.023 mag. Similarly, in Fig. 3(b) we compare the CCD V magnitudes with the photoelectric values of Stetson (1981) for stars in NGC 1851. The (unweighted) mean difference is 0.004 mag with a standard deviation of 0.018 mag.

The agreement with the photoelectric measures of Demers (1969) for M2, however, is not as satisfactory. The mean difference for the ten stars in common is -0.044 mag with a standard deviation of the differences of 0.052 mag. Similarly, for the eight M15 stars in common with the photoelectric photometry of Sandage (1970), the mean difference in the V magnitudes is comfortably small at 0.006 mag but $\sigma(\text{diff}) = 0.050$ mag. We believe that these large $\sigma(\text{diff})$ reflect more the difficulty of doing conventional photometry in crowded cluster fields than they do errors in the CCD photometry. Indeed in a number of cases the large differences result from the presence of faint nearby companions which

TABLE IV. M2 photometry.

Star	<i>V</i>	<i>V-I</i>	<i>N</i> _{obs}	Star	<i>V</i>	<i>V-I</i>	<i>N</i> _{obs}	Star	<i>V</i>	<i>V-I</i>	<i>N</i> _{obs}
A ¹	13.207	1.464	3	I-401	15.953	0.991	2	A I-23	13.667	1.317	1
B	14.049	1.192	1	I-451	15.858	0.992	2	A I-33	15.622	0.854	2
G	14.620	1.117	3	I-452	14.554	1.121	2	A II-19	13.984	1.234	2
H	15.948	0.979	2	I-461	15.214	0.939	2	A II-22	15.706	0.981	3
K	15.756	0.998	2	I-481	15.846	0.962	2	A II-24	15.256	0.951	1
L	14.037	1.166	4	I-511	14.842	1.090	2	A II-59	13.296	1.437	3
M	14.890	1.074	2	I-514	15.927	0.974	2	A II-65	15.090	1.048	1
Q	13.199	1.431	2	I-517	15.961	0.977	2	A IV-20	14.042	1.227	2
S	13.727	1.284	3	I-546	15.830	0.974	2	A IV-21	15.195	1.032	2
T	13.783	1.283	3	I-569	16.314	0.985	1	A IV-22	14.348	1.183	1
I-2	14.027	1.228	1	I-574	15.611	1.020	1	A IV-26	15.803	1.007	2
I-8	14.369	1.187	2	I-576	13.393	1.378	3	A IV-36	15.129	0.963	3
I-17	14.820	0.636	1	I-578	15.963	0.989	1	A IV-42	14.092	1.119	2
I-20	15.167	1.029	1	I-579	14.072	0.393	1	A IV-52	14.809	1.085	3
I-21	15.106	1.113	2	I-583	15.256	0.908	1	-61+70 ⁴	14.218	1.331	4
I-26	15.025	0.981	2	I-586	14.855	1.096	2	-56-56	13.308	1.411	1
I-48	15.927	0.994	1	I-587	15.153	0.154	1	-46+60	13.081	1.575	3
I-51	15.523	0.995	2	I-588	16.022	0.942	1	-37+75	15.832	0.765	3
I-53	14.976	1.085	2	I-589	14.884	0.806	1	-30-32	13.062	1.520	1
I-100	15.662	1.105	1	I-590	15.148	0.762	1	-25+135	14.265	1.103	3
I-103	13.474	1.368	3	I-591	14.791	1.099	1	-13+87	13.933	1.240	2
I-104	13.909	1.246	3	I-594	16.240	0.964	1	-05+79	13.118	1.538	1
I-105	15.456	1.036	1	II-10	14.516	1.137	1	-01-41	12.941	1.558	1
I-323	15.751	0.976	1	II-105	16.727	0.981	1	+04-80	13.920	1.230	1
I-334	15.162	1.058	3	II-110	13.961	0.982	1	+22+22	13.224	1.444	1
I-335	15.083	1.076	1	II-114	15.298	0.969	1	+36-18	13.040	1.460	1
I-384	16.062	0.235	2	II-119	16.262	0.989	1	+38-48	15.162	0.949	3
I-391	15.151	0.887	3	II-132	16.015	0.866	1	+42-42	13.835	1.257	2
I-393	15.717	0.998	2	AC11 ²	12.937	1.584	1	+49+17	13.076	1.440	1
I-394	16.345	0.910	2	AC14	13.159	1.542	1	+52-48	15.257	1.040	3
I-395	14.326	1.178	2	AC125	13.124	1.393	1	+75-40	13.547	1.334	3
I-398	16.584	0.917	2	AC133	12.904	1.475	1	+97-68	13.932	1.155	1
I-399	16.155	0.952	1	AC701	13.211	1.629	1				
I-400	16.133	0.188	1	A I-22 ³	14.964	1.070	2				

¹Single letter, I- and II- star numbers from Harris (1975).²Star numbers from Auriere and Cordoni (1983).³Star numbers from Arp (1955).⁴Star numbers are of the form +x+y where x and y are positions in arcsec relative to the cluster center on the system of Pryor *et al.* (1986). The positive x direction is East, positive y North.

TABLE V. NGC 6397 photometry.

Star	V	$V-I$	N_{obs}
RGO43 ^a	10.924	1.328	1
RGO211	10.101	1.604	1
RGO428	11.507	1.283	1
RGO468	11.508	1.290	2
RGO469	9.957	1.628	1
RGO574	12.736	1.171	1
RGO603	10.361	1.476	1
RGO666	11.261	0.832	1
RGO669	10.524	1.440	1
RGO698	10.222	1.570	1
A97 ^b	12.528	1.213	1
A163	12.563	1.200	1
A200	12.806	1.144	1
A302	10.401	1.502	1
A305	11.685	1.255	1
A314	12.275	1.201	1
A337	12.609	1.162	1
A340	9.987	1.382	2
A344	13.275	2.141	1
A345	12.541	1.175	1

^aStar numbers from Woolley *et al.* (1961).^bStar numbers from Alcaino (1977).

would have been included in the aperture of a conventional photometer but which can be seen and excluded in the CCD measurements.

Independently calibrated CCD photometry is also available for both Pal 12 (Stetson *et al.* 1989) and Eridanus (Da Costa 1985). It is therefore of some interest to compare our

TABLE VI. M15 photometry.

Star	V	$V-I$	N_{obs}	Star	V	$V-I$	N_{obs}
P13 ^a	14.292	1.143	1	II-42	13.288	1.333	4
S1	13.067	1.385	2	II-51	15.192	1.061	2
S3	13.482	1.292	1	II-64	13.521	1.287	3
S6	13.442	1.343	3	II-75	13.084	1.407	3
S19	14.807	1.129	3	II-77	15.191	0.991	2
X1	13.980	0.711	1	IV-11	15.327	1.073	2
X1-SW	14.723	0.863	1	IV-25	15.409	1.028	1
X1-NW	15.705	0.614	1	B90 ^d	13.806	1.239	1
X2	14.640	1.144	1	B137	14.966	1.019	2
X2-SE	15.749	1.025	1	B129	14.486	0.740	2
X5	13.680	1.047	1	B187	14.291	1.169	3
X5-NE	15.864	1.041	1	B192	15.216	1.092	2
X6	14.164	1.158	1	B211	14.530	1.130	2
X7	13.449	0.862	1	B213	15.107	1.112	2
I-6 ^b	13.893	1.179	4	B239	14.373	0.107	3
I-12	12.776	1.525	4	B245	14.579	1.138	4
I-23	14.544	1.147	2	B260	14.452	1.178	4
I-38	14.363	1.128	3	B302	14.196	1.211	3
I-41	14.203	1.202	4	B355	15.034	1.093	2
I-43	13.936	1.227	5	B363	13.863	1.251	3
I-50	13.651	1.294	5	B371	14.633	1.149	3
I-57 ^c	14.956	1.621	3	K240 ^e	12.960	1.411	4
I-62	14.518	1.139	1	K319	13.559	1.224	4
I-63	14.367	1.170	1	K366	14.295	1.104	1
I-65	15.208	1.055	2	K386	12.795	1.461	4
I-72	15.236	0.981	3	K764	13.848	1.222	3
I-74	14.059	1.222	5	K809	14.900	1.057	1
II-16	13.760	1.229	2	K810	14.490	1.173	1
II-29	13.310	1.345	4	K853	12.907	1.443	4
II-30	13.445	1.297	4	K863	14.027	1.173	1
II-31	13.334	1.326	4				

^aStar numbers from Sandage (1970) except for those identified by a Sandage (1970) number and a direction. The direction is relative to the designated Sandage star; the stars are visible on the Sandage (1970) charts.^bStar numbers from Arp (1955).^cComparison of CCD and transformed Kustner (1921) positions indicates significant proper motion, not a cluster member.^dStar numbers from Buonanno *et al.* (1983).^eStar numbers from Kustner (1921).

TABLE VII. Pal 12 photometry.

Star ^a	V	$V-I$	N_{obs}
1	14.571	1.608	4
1106	17.645	1.200	1
1118	14.842	1.490	4
1128	15.445	1.303	4
1140	16.329	0.956	4
1218	17.128	0.886	4
1219	17.659	0.968	1
1224	17.135	0.905	4
1305	15.860	1.166	4
1314	17.745	0.930	1
1317	16.887	1.059	4
1329	17.040	0.907	4
1337	16.675	1.024	4
2111	16.994	0.906	4
2125	17.114	0.909	4
2224	17.623	0.988	1
2422	16.314	0.705	4
3111	17.128	0.898	1
3126	17.283	1.031	1
3460	16.705	0.929	4

^aStar numbers from Harris and Canterna (1980).

photometry with these sources, though once again the comparison must be restricted to the V magnitudes. The results are shown in Figs. 3(c) and 3(d). For Pal 12 the agreement is exceedingly good, with the mean difference for the 17 stars in common with the Stetson *et al.* (1989) study being only -0.003 mag with $\sigma(\text{diff}) = 0.008$ mag! For Eridanus, the corresponding numbers for the 15 stars in common with Da Costa (1985) are 0.023 and 0.016 mag. Thus there is some indication of a possible small zero-point offset in the Da Costa (1985) V photometry, but the scatter is encouragingly small.

As a consequence of these comparisons, we believe that the CCD photometry presented here is accurately on the standard system and that it is as precise as the best available conventional photoelectric photometry. Yet many more stars have been observed in a much smaller amount of telescope time than would have been required to accumulate the same data by conventional means. Such is the power of a high quantum efficiency, panoramic, linear detector!

TABLE VIII. Eridanus photometry.

Star ^a	V	$V-I$	N_{obs}
4	18.969	1.137	2
7	19.841	2.570	1
12	19.067	1.209	2
16	19.901	0.987	1
17	18.729	1.145	2
19	19.306	1.117	1
20	19.013	1.127	2
25	18.419	1.215	2
26	18.358	1.228	2
27	18.663	1.174	2
28	19.030	1.015	2
31	17.632	1.482	2
32	19.630	1.002	1
33	19.347	0.993	1
41	20.025	0.834	1

^aNumbers from Da Costa (1985).

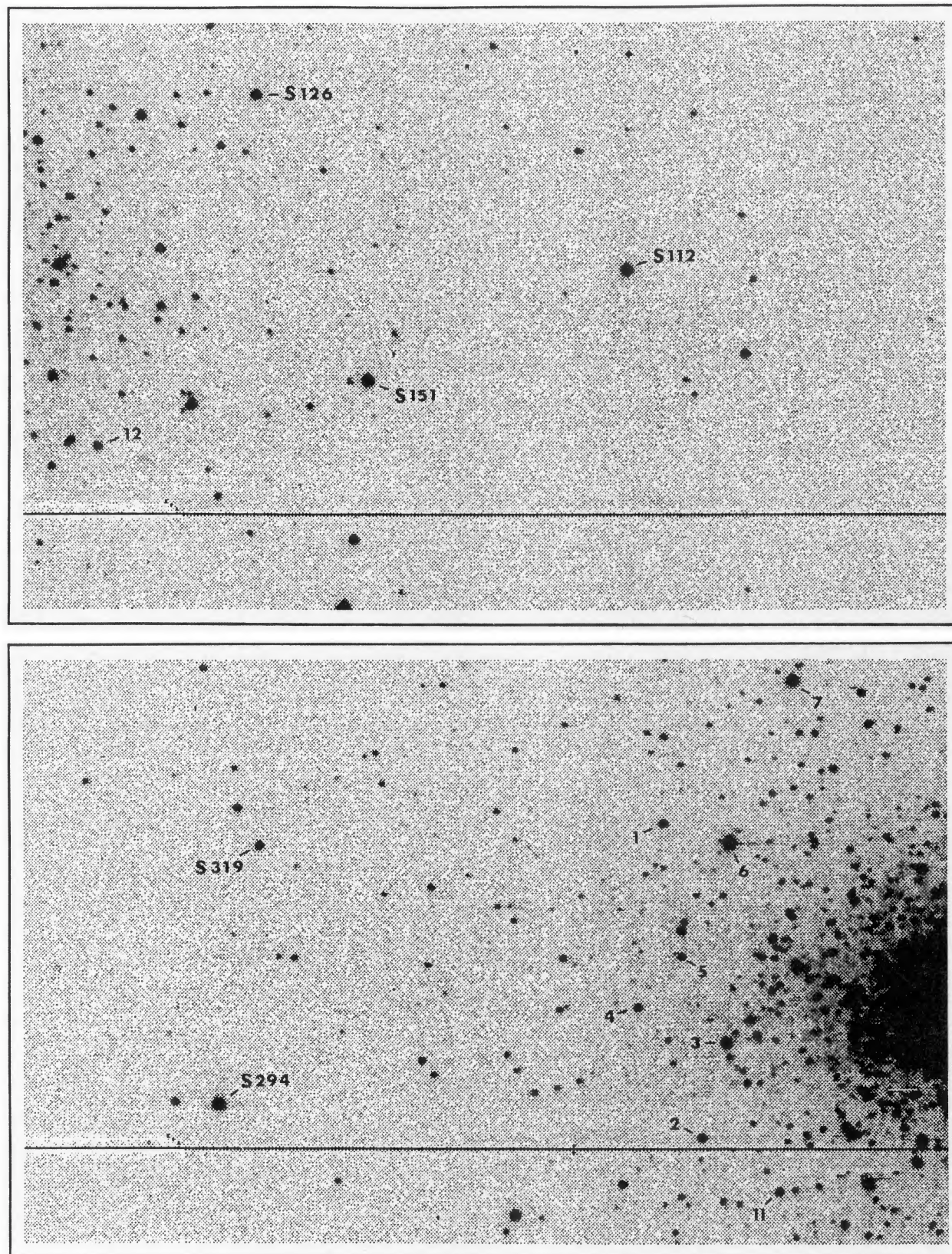


FIG. 1. Finding charts for previously unidentified stars in NGC 1851. In both panels North is at the top and East is to the right. Star numbers preceded by an S come from Stetson (1981) and both panels are from gray-scale plots of 15 s *I* exposures. The N-S panel boundary is 165" in length.

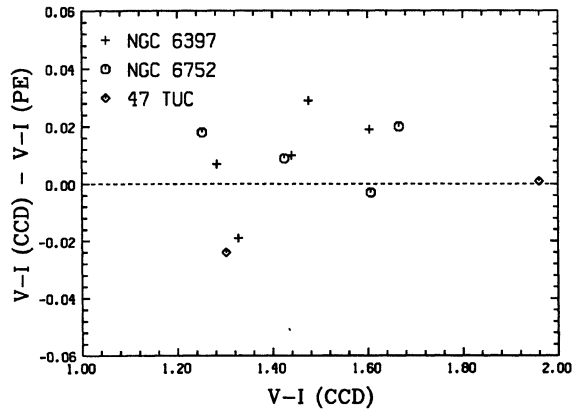


FIG. 2. Comparison of the CCD $V-I$ colors with those determined by conventional photoelectric photometry for the clusters NGC 6397, NGC 6752, and 47 Tuc. The sources of the photometry are given in the text.

III. RESULTS

$a) (M_V, (V-I)_0)$ Diagram

In Fig. 4 $c-m$ diagrams derived from the CCD V, I photometry are presented for the six standard clusters studied. The photometry extends in each cluster from the tip of the giant branch (with the exception of 47 Tuc; see below) to approximately the level of the horizontal branch. Indeed red horizontal branch (HB) stars are present in the $c-m$ diagrams of NGC 1851 and 47 Tuc near the faint limit of the data. Also shown in Fig. 4 are curves derived from low-order polynomial fits to the cluster photometry. In making these fits, stars that lie off the giant branch have been excluded.

These stars are principally AGB stars, red HB stars, and the occasional field star.

It is evident, however, that the points shown in Fig. 4 for 47 Tuc are not sufficiently numerous to constrain the giant branch fit. We have therefore made use of the 47 Tuc photometry available in Armandroff (1988) and Lloyd Evans (1983) to augment our data. The complete dataset is shown in Fig. 5, where it is clear from the intermingling of the points from the three sources that there are no systematic differences between the sets of photometry. The brightest and reddest stars in this cluster are all variables and we have included in Fig. 5 those variables for which Lloyd Evans (1983) gives at least three measures; the stars are plotted at their mean magnitude and color.

To convert these fiducial giant branch curves to the $(M_V, (V-I)_0)$ plane, a distance scale and cluster reddenings must be adopted. While the reddenings for these clusters are all relatively small and well known, the question of the appropriate distance scale remains controversial. In this paper we have adopted the distance scale that results from the theoretical horizontal branch models of Lee, Demarque, and Zinn (1990) (hereafter referred to as LDZ). For these calculations, the luminosity of globular cluster RR Lyrae variables follows the relation $M_V(\text{RR}) = 0.82 + 0.17[\text{Fe}/\text{H}]$. The variation of luminosity with abundance contained in this relation, which is appropriate for a helium abundance $Y = 0.23$, agrees to within the uncertainties with that derived from the application of Baade-Wesselink techniques to field RR Lyraes (see LDZ for a complete discussion). Application of this relation to 47 Tuc, however, is complicated by the lack of RR Lyrae stars in this cluster. To compensate for this deficiency, the theoretical HB models have again been used; Lee, Demarque, and Zinn (1987) show that the red HB stars in 47 Tuc are 0.1–0.2 mag brighter than the nonexistent cluster RR Lyrae variables. Consequently, in deriving the distance modulus of 47 Tuc from the LDZ rela-

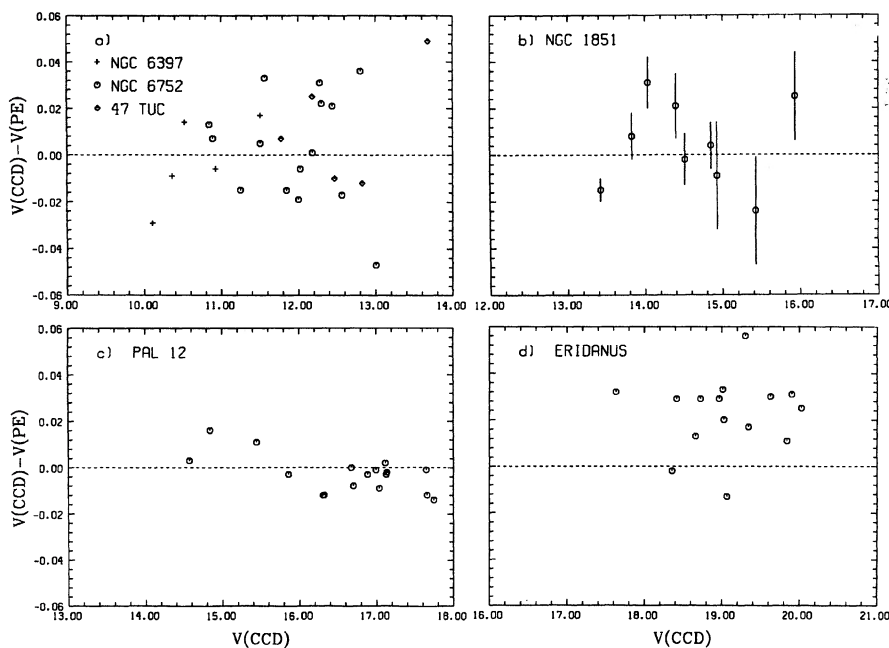


FIG. 3. Comparison of the CCD V magnitudes with (a) conventional photoelectric photometry of stars in NGC 6397, NGC 6752, and 47 Tuc, (b) conventional photoelectric photometry of stars in NGC 1851 [the error bars are the uncertainties in the photoelectric V magnitudes as listed by Stetson (1981)], (c) CCD photometry of stars in Pal 12, and (d) CCD photometry of stars in Eridanus. The sources of the photometry are given in the text.

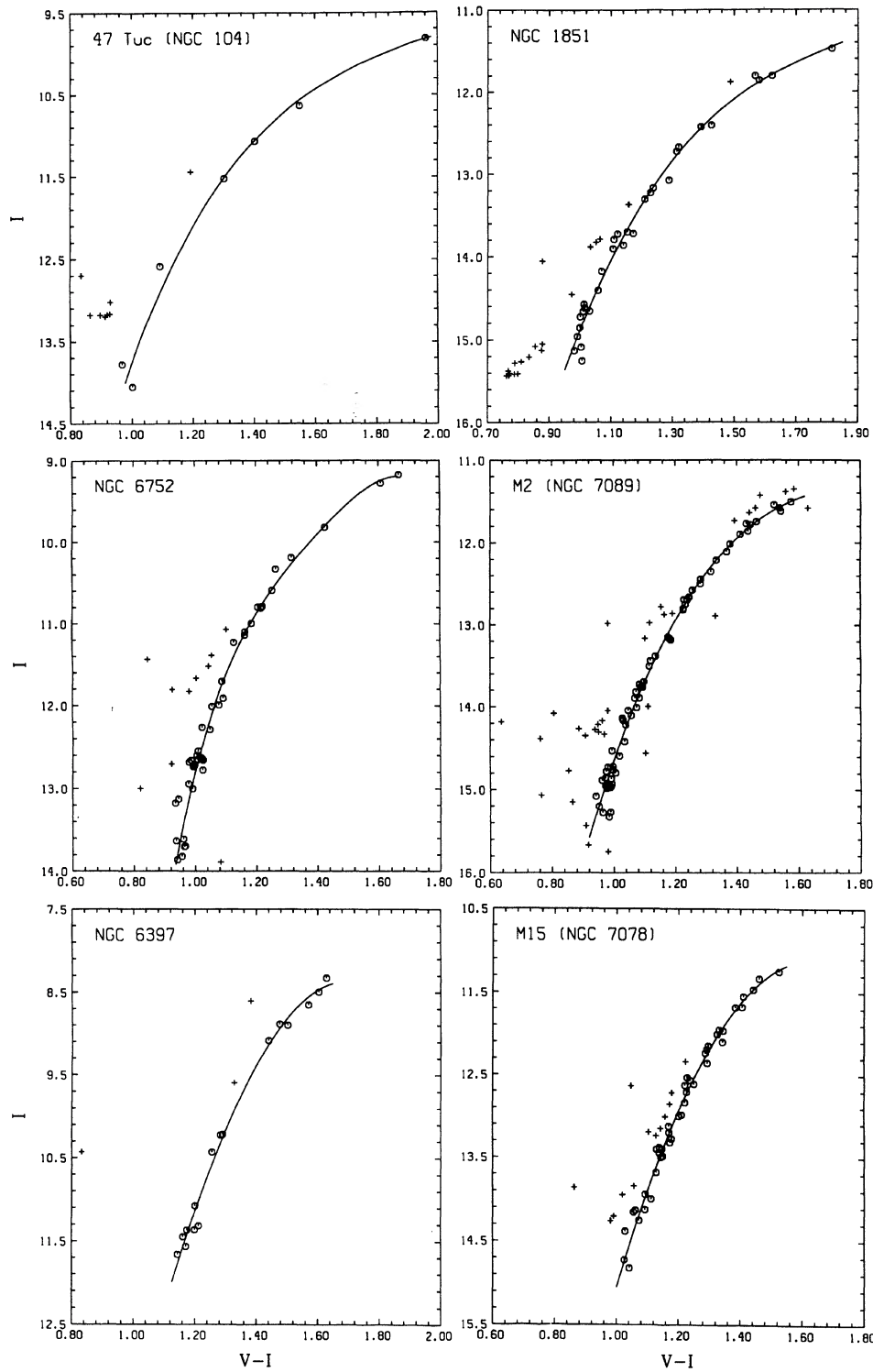


FIG. 4. (I , $V-I$) giant branches for the clusters 47 Tuc (NGC 104), NGC 1851, NGC 6752, M2 (NGC 7089), NGC 6397, and M15 (NGC 7078) determined from the CCD photometry. Except for 47 Tuc (see Fig. 5) the solid curves are polynomial fits to the open symbols; stars represented by plus symbols were not included in the fits.

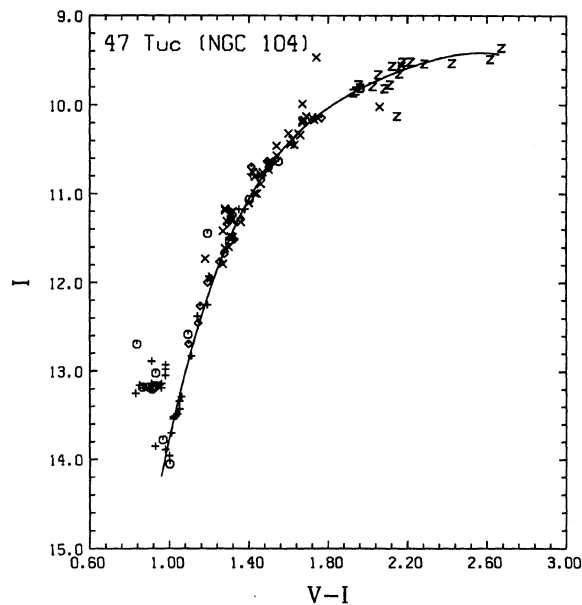


FIG. 5. Complete dataset on which the 47 Tuc giant branch, shown by the solid line, is based. Open symbols are the CCD measures presented here while plus symbols are from the CCD photometry of Armandroff (1988). The \times and Z symbols represent the conventional photoelectric photometry of Lloyd Evans (1983) and are used to plot nonvariable and variable stars, respectively. The variables are shown at the mean magnitudes and colors of the Lloyd Evans photometry.

tion, we have made an adjustment of 0.15 mag to the predicted RR Lyrae absolute magnitude. The resulting distance modulus $(m - M)_{app, V} = 13.51$ agrees well with that (13.4) used by Hesser *et al.* (1987) in their study of the age of this cluster. We note that the clusters NGC 6397 and NGC 6752 also do not contain RR Lyrae stars, but for these clusters the HB apparent magnitudes used come from fitting the cluster blue horizontal branches to those of clusters with slightly redder horizontal branches containing RR Lyrae stars (see, for example, Cannon 1974).

The reddenings and horizontal branch apparent magnitudes, taken from Armandroff (1989), are given for each cluster in Table IX together with the adopted HB absolute magnitudes, based on the LDZ relation, and the resulting distance moduli. Figure 6 then displays the resulting $(M_I, (V - I)_0)$ diagram, in which the giant branches for all six clusters are shown. Sample points for each giant branch are given in Table X. In constructing this diagram we have used the $E(V - I)/E(B - V)$ relation of Dean, Warren, and Cousins (1978), with $(B - V)_0$ taken as 1.20 for all stars. This latter assumption does not affect the calculated $E(V - I)$ values.

b) Comparison with MKD

We now turn to a discussion of the uses of Fig. 6. First, however, we comment on the differences between this diagram and the equivalent one given in MKD. The principal difference results from the distance scales adopted in each: MKD used a scale in which $M_V(\text{HB}) = +0.6$ for metal-poor clusters and $M_V(\text{HB}) = +0.9$ for 47 Tuc. Thus, in the

TABLE IX. Adopted globular cluster parameters.

Cluster	[Fe/H]	$E(B - V)$	$V(\text{HB})$	$M_V(\text{RR})$	$(m - M)_{app, V}$
47 Tuc	-0.71	0.04	14.06	0.70	13.51 ^a
NGC 1851	-1.29	0.02	16.05	0.60	15.45
NGC 6752	-1.54	0.04	13.75	0.56	13.19
M2	-1.58	0.02	16.05	0.55	15.50
NGC 6397	-1.91	0.18	12.90	0.50	12.40
M15	-2.17	0.10	15.86	0.45	15.41
NGC 362	-1.28	0.06	15.43	0.60	14.83
M5	-1.40	0.03	15.15	0.58	14.57

^aRed horizontal branch stars assumed to be 0.15 mag brighter than $M_V(\text{RR})$ for this cluster (Lee, Demarque, and Zinn 1987).

MKD calibration, the giant branches are 0.15 mag fainter at constant color for the most metal-poor clusters and approximately 0.35 mag fainter for 47 Tuc. Other than this systematic difference, however, the agreement between the MKD giant branches and those derived here is quite satisfactory. This agreement is shown in Fig. 7, where we plot the giant branches for M15, NGC 6397, NGC 6752, and 47 Tuc from Fig. 6 together with the equivalent MKD data shifted in M_I [and in $(V - I)_0$ when different reddenings were assumed] to compensate for the different distance scale [and small differences in the $V(\text{HB})$ values used]. As Fig. 7 illustrates, the agreement for 47 Tuc is excellent; only near the tip of the giant branch is the MKD curve slightly fainter. For NGC 6752 the MKD curve is systematically redder by ~ 0.03 mag while the agreement for NGC 6397 is again excellent. Note, however, that in MKD the giant branches of M92 and NGC

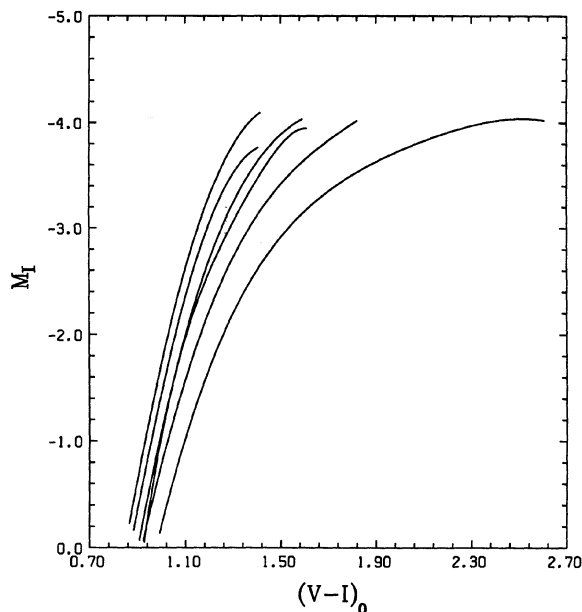


FIG. 6. Giant branch loci in the $(M_I, (V - I)_0)$ plane for the clusters (left to right) M15, NGC 6397, M2, NGC 6752, NGC 1851, and 47 Tuc, respectively. The absolute I magnitudes are on the distance scale of Lee, Demarque, and Zinn (1990), in which $M_V(\text{RR}) = 0.82 + 0.17[\text{Fe}/\text{H}]$.

TABLE X. Representative giant branch points.

$(V-I)_o$	M_T	$(V-I)_o$	M_T	$(V-I)_o$	M_T	$(V-I)_o$	M_T
(a) M15 (NGC 7078)							
0.866	-0.224	0.965	-1.362	1.091	-2.535	1.240	-3.508
0.882	-0.427	0.981	-1.533	1.113	-2.707	1.273	-3.664
0.899	-0.625	1.003	-1.753	1.135	-2.869	1.317	-3.840
0.915	-0.817	1.025	-1.963	1.157	-3.021	1.350	-3.947
0.932	-1.004	1.047	-2.163	1.179	-3.164	1.377	-4.020
0.948	-1.186	1.069	-2.354	1.207	-3.329	1.416	-4.095
(b) NGC 6397							
0.884	-0.162	0.990	-1.338	1.138	-2.627	1.286	-3.458
0.899	-0.351	1.011	-1.549	1.159	-2.775	1.308	-3.536
0.915	-0.536	1.032	-1.751	1.180	-2.913	1.329	-3.604
0.931	-0.716	1.053	-1.944	1.202	-3.042	1.350	-3.662
0.947	-0.892	1.074	-2.128	1.223	-3.161	1.371	-3.709
0.958	-1.007	1.096	-2.304	1.244	-3.270	1.392	-3.745
0.974	-1.175	1.117	-2.470	1.265	-3.369	1.408	-3.765
(c) M2 (NGC 7089)							
0.914	-0.151	1.075	-1.780	1.271	-3.088	1.467	-3.807
0.928	-0.315	1.103	-2.009	1.299	-3.223	1.488	-3.856
0.942	-0.475	1.131	-2.223	1.327	-3.346	1.509	-3.900
0.963	-0.706	1.159	-2.423	1.355	-3.459	1.530	-3.940
0.991	-0.999	1.187	-2.609	1.383	-3.560	1.551	-3.976
1.019	-1.275	1.215	-2.781	1.411	-3.652	1.572	-4.007
1.047	-1.536	1.243	-2.941	1.439	-3.734	1.593	-4.035
(d) NGC 6752							
0.935	-0.170	1.072	-1.741	1.269	-2.910	1.474	-3.708
0.950	-0.399	1.094	-1.920	1.300	-3.044	1.497	-3.774
0.965	-0.612	1.117	-2.083	1.330	-3.173	1.520	-3.833
0.980	-0.810	1.148	-2.279	1.360	-3.297	1.543	-3.881
1.003	-1.081	1.178	-2.456	1.391	-3.416	1.566	-3.918
1.026	-1.324	1.208	-2.618	1.421	-3.529	1.588	-3.941
1.049	-1.543	1.239	-2.768	1.452	-3.635	1.611	-3.948
(e) NGC 1851							
0.932	-0.150	1.184	-2.119	1.436	-3.226	1.652	-3.744
0.986	-0.662	1.220	-2.322	1.472	-3.333	1.688	-3.808
1.040	-1.121	1.256	-2.508	1.508	-3.431	1.724	-3.868
1.076	-1.400	1.310	-2.759	1.544	-3.520	1.760	-3.925
1.112	-1.659	1.364	-2.978	1.580	-3.601	1.796	-3.980
1.148	-1.898	1.400	-3.108	1.616	-3.675	1.823	-4.021
(f) 47 Tuc (NGC 104)							
0.991	-0.131	1.467	-2.814	1.943	-3.675	2.351	-3.998
1.060	-0.717	1.535	-3.001	2.011	-3.745	2.402	-4.019
1.127	-1.220	1.603	-3.160	2.079	-3.809	2.453	-4.033
1.195	-1.651	1.671	-3.294	2.147	-3.866	2.504	-4.039
1.263	-2.018	1.739	-3.410	2.198	-3.905	2.538	-4.038
1.331	-2.329	1.807	-3.510	2.249	-3.940	2.572	-4.032
1.399	-2.592	1.875	-3.597	2.300	-3.971	2.606	-4.021

6397 were not distinguished because of the small number of stars available; the combined giant branch was taken as that appropriate for the abundance of M92. Consequently, as Fig. 7 shows, the M15/M92 abundance giant branch is approximately 0.04 mag bluer in these new data than in the MKD calibration. These differences are sufficiently small, however, that results based on the MKD calibration do not require reinterpretation, though it should always be kept in mind that abundances derived from the calibration of Fig. 6 or the equivalent MKD diagram are sensitive to the assumed distance scale. For example, use of Fig. 6 instead of the diagram in MKD will result in higher abundances for redder $(V-I)_0$ colors because of the more luminous 47 Tuc giant branch.

c) Abundance Calibration

In addition to the six clusters discussed here, the photometry of Lloyd Evans (1983) is extensive enough for M5 and NGC 362 that these clusters can also be included in the discussion. Their giant branches, determined in the same way as for the other clusters, are shown in Fig. 8, while Fig. 9 shows the $(M_I, (V-I)_0)$ plane for all eight clusters. The parameters assumed to place M5 and NGC 362 in this diagram are also given in Table IX. With this sample we can now investigate the abundance sensitivity of the $(M_I, (V-I)_0)$ diagram. A superficial glance at Fig. 9 re-

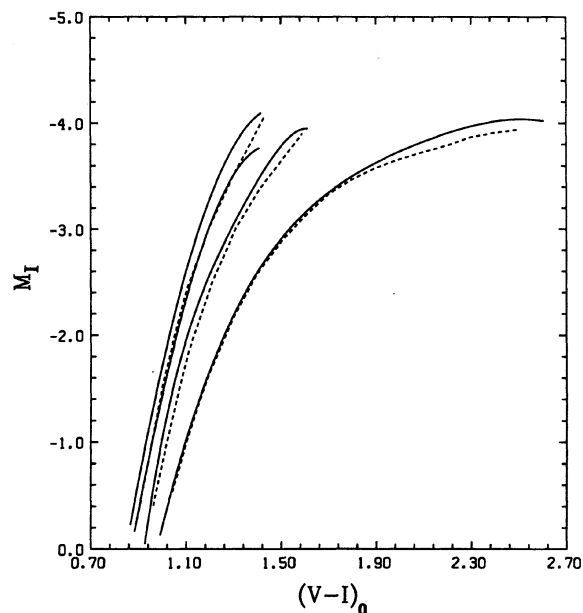


FIG. 7. Comparison of the $(M_I, (V-I)_0)$ giant branch loci presented here (solid curves) with those given in Mould, Kristian, and Da Costa (1983). The MKD data (dashed curves) have been shifted in M_I to compensate for the different distance scales assumed and in $(V-I)_0$ if different reddenings were used. The solid curves are, respectively, the giant branches of M15, NGC 6397, NGC 6752, and 47 Tuc, while the dashed curves are the MKD giant branches for M92/NGC 6397, NGC 6752, and 47 Tuc.

veals that the greatest sensitivity occurs for higher luminosities. On the other hand, sparse clusters such as Pal 12 and Eridanus, which will be discussed in the next section, may have giant branches that are not populated at the highest luminosities. As a compromise, we show in Fig. 10 the intrinsic $(V-I)_0$ color of the giant branch, at an absolute I magnitude of $M_I = -3.0$, as a function of $[Fe/H]$ for the eight clusters of Fig. 9. The abundances are taken from Armandroff (1989), and their uncertainty from either Arman-

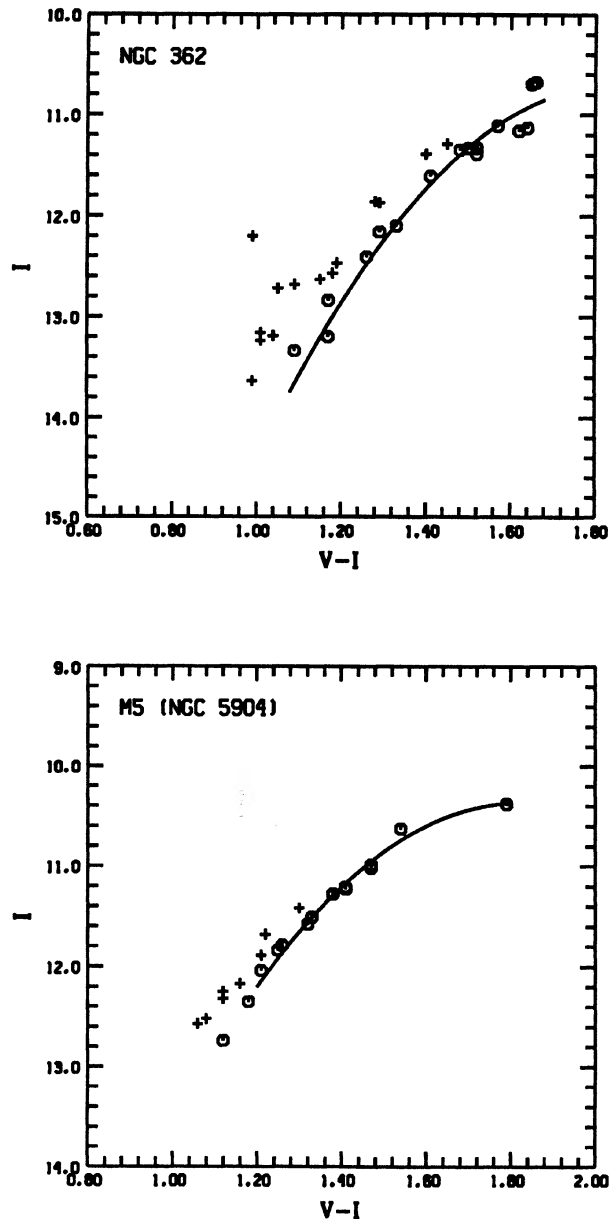


FIG. 8. $(I, V-I)$ giant branches for the globular clusters NGC 362 (upper panel) and M5 (NGC 5904) (lower panel) from the photometry of Lloyd Evans (1983). The solid curves are polynomial fits to the open symbols and are taken as defining the cluster giant branches.

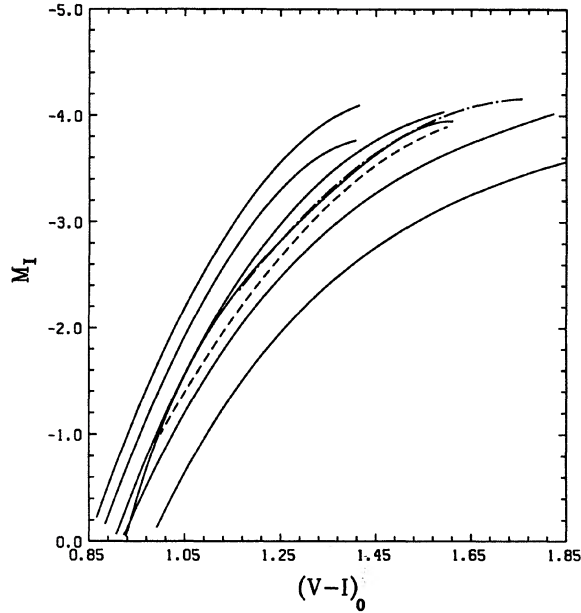


FIG. 9. Giant branch loci in the $(M_I, (V-I)_0)$ plane of the six standard clusters from Fig. 6 (solid curves) together with the giant branches of M5 (dotted-dashed curve) and NGC 362 (dashed curve) placed in the diagram in the same way as the standard clusters. Note that the $(V-I)_0$ scale differs from that of Fig. 6 to allow the curves to be more readily distinguished.

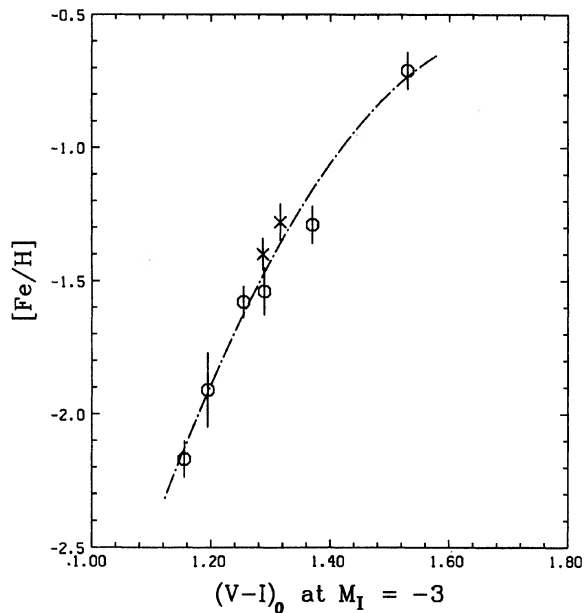


FIG. 10. Abundance calibration: $[\text{Fe}/\text{H}]$ values from the literature, together with their associated uncertainties, are plotted against the $(V-I)_0$ color of the giant branch at an absolute I magnitude $M_I = -3.0$. The open symbols are the six standard clusters presented here, while the \times symbols represent M5 and NGC 362, whose photometry comes from Lloyd Evans (1983). The dotted-dashed curve is an unweighted second-order polynomial fit to these data.

droff and Zinn (1988) or Zinn and West (1984). These abundances are also tabulated in Table IX. An excellent correlation is present and the dispersion about the fitted curve is only 0.07 dex, scarcely larger than the mean abundance uncertainty! This curve is defined by the relation

$$[\text{Fe}/\text{H}] = -15.16 + 17.0(V-I)_{0,-3} - 4.9[(V-I)_{0,-3}]^2, \quad (1)$$

where $(V-I)_{0,-3}$ is the giant branch color at $M_I = -3$. A linear fit to the points of Fig. 10 is noticeably inferior. The small dispersion about the fitted line in Fig. 10 indicates that good relative abundances can be derived from V, I photometry. We must, however, emphasize once again that this technique produces only relative abundances: a different distance scale and/or different abundances for the calibrating clusters will change the calibration. Further, at present the calibration is defined only up to the abundance of 47 Tuc, though we plan to extend it to higher abundances by obtaining V, I photometry of more metal-rich clusters.

The largest deviation from the fitted curve in Fig. 10 is shown by the cluster NGC 1851, which appears to have too red a giant branch for the abundance and reddening given in Table IX. However, we do not regard this deviation as significant for two reasons. First, integrated spectra at the infrared Ca II triplet (Armandroff and Zinn 1988) suggest that NGC 1851 may in fact be more metal rich than the abundance given in Table IX, by some 0.15 dex or so. Such an abundance increase would place the cluster on the curve in Fig. 10. Alternatively, it is possible that the reddening for NGC 1851 is larger than that given in Table IX [which is due to Stetson (1981)]. Zinn (1980) gives $E(B-V) = 0.06$ mag from his integrated Q39 photometry, while Da Costa (1982), on the basis of the strength of the interstellar K line in the spectrum of the B-type UV-bright cluster star UV5, also suggested that the NGC 1851 reddening is larger than 0.02 mag. An increase in the NGC 1851 reddening of 0.03 mag, corresponding to $\Delta(V-I)_0$ of -0.04 mag, is also sufficient to move NGC 1851 onto the calibration curve in Fig. 10.

We further note that the location of M5 in Fig. 10 is inconsistent with the higher abundance for this cluster, $[\text{Fe}/\text{H}] = -1.13 \pm 0.11$ dex, advocated by Richer and Fahlman (1987). Their value is derived from an estimate of $\delta(U-B)_{0.6}$ determined from CCD UBV photometry, though the relation of this parameter to abundance for globular clusters is, as they themselves admit, not well established.

We conclude therefore that ranking clusters by the $(V-I)_0$ colors of their giant branch stars is a reliable technique for determining relative metal abundances. We note also that while the calibration presented here is strictly valid for stellar populations comparable in age to the calibrating galactic globular clusters, it appears that the age sensitivity is not large. Using the Revised Yale Isochrones (Green, Demarque, and King 1987) as a guide, the difference in $(V-I)_{0,-3}$ between a 7 Gyr and a 15 Gyr giant branch at $Z = 0.001$ ($[\text{Fe}/\text{H}] = -1.3$ dex) is only 0.05 mag (with the younger being bluer), yielding an abundance "error" of 0.2 dex based on Eq. (1). Thus it appears the calibration is applicable to any population in which the bulk of the stars are more than a few Gyr old without introducing significant systematic errors.

Before employing this calibration to determine abundances for particular clusters, however, we can make use of it and the precision of the CCD photometry described above to set limits on the abundance dispersion within each cluster of those elements (principally low-ionization potential metals) that control the effective temperature of the giant branch. Only ω Cen, and perhaps also M22, are known to contain significant internal abundance ranges in these elements, and the lack of such internal abundance ranges among the globular cluster population is often used as an argument against self-enrichment at the time of cluster formation (e.g., Larson 1988). The curves shown in Fig. 4 were determined by least-squares polynomial fits using $V-I$ color as the independent variable. The procedure can be reversed, however, and by using the I magnitudes as the independent variable a standard deviation in $V-I$ color about the fitted curve results. We can then compare this standard deviation with that expected from the errors in the $V-I$ colors to place limits on the intrinsic $V-I$ spread on the cluster giant branch. This limit, in turn, constrains the intrinsic abundance spread within the cluster, where here, and for the rest of this section, "abundance" is understood to mean those elements that control the giant branch effective temperature.

The $V-I$ standard deviation about the fitted curves is tabulated in Table XI for the six principal calibrating clusters [NGC 362 and M5 are not included here because we have no explicit knowledge of the errors in the Lloyd Evans (1983) photometry]. For 47 Tuc, we have restricted the fit to stars with $V-I < 2$ since the variables, by their very nature, introduce dispersion into the fitted relation. Also given in the table are the number of stars incorporated in the fit. The dispersions in the table are quite small, and given the discussion of the errors in the CCD photometry above, we conclude that they are due entirely to the photometric errors; i.e., the results are consistent with intrinsic color widths of zero. Alternatively, if we regard the dispersions given in Table XI as 3σ upper limits on the intrinsic color width of each cluster giant branch, then using the differential of Eq. (1) and the appropriate $(V-I)_{0,-3}$ values (there appears to be no systematic change in the observed widths with I magnitude), the corresponding 3σ upper limits on the abundance range in each cluster are 0.04, 0.07, 0.05, 0.06, 0.06, and 0.09 dex, respectively, for 47 Tuc, NGC 1851, NGC 6752, M2, NGC 6397, and M15. The small size of these upper limits indicates once again that most globular clusters are extremely homogeneous with respect to the abundances of the elements that control the giant branch effective temperature. We also note that the lack of significant change in the observed widths with increasing I magnitude, despite the increased ease of separation of AGB and red giant branch

stars it allows, indicates that the results have not been unduly influenced by our choices of stars to include in the giant branch fits.

d) Abundances of Pal 12 and Eridanus

In Fig. 11 the Pal 12 photometry is plotted in the $(M_I, (V-I)_0)$ plane together with the giant branches for M15, M2, NGC 1851, and 47 Tuc. Since use of the LDZ distance scale requires *a priori* knowledge of the abundance of a system, the Pal 12 points were placed in this figure by an iterative procedure. First, an initial abundance estimate is used to calculate a horizontal branch absolute visual magnitude on the LDZ scale (note that we have chosen not to modify this HB absolute magnitude, as was done for 47 Tuc, to compensate for the presence of only red HB stars in Pal 12, since there is no obvious justification for doing so). Then, with an adopted reddening of $E(B-V) = 0.02$ mag and taking $V(\text{HB}) = 17.10$ (Armandroff 1989), the Pal 12 stars can be placed in the $(M_I, (V-I)_0)$ diagram. This in turn yields an abundance relative to the calibrating clusters and thus a new $M_V(\text{HB})$ on the LDZ scale. The procedure is repeated until consistency is obtained.

Since the upper part of the Pal 12 giant branch is defined by only four stars, we have not attempted to define $(V-I)_{0,-3}$ for this cluster to determine the abundance via Eq. (1). Instead we have simply measured at constant M_I the location relative to the NGC 1851 and 47 Tuc giant branches of the six giants with $(V-I)_0 > 0.96$ in Fig. 11. Adopting the abundances for these calibrating clusters given in Table IX then yields an "abundance" for each individual Pal 12 giant. These individual determinations were then combined by taking a weighted average; the weight being the

TABLE XI. Giant branch color dispersions.

Cluster	N (stars)	$\sigma(V-I)$ (mag)
47 Tuc	69	0.020
NGC 1851	29	0.020
NGC 6752	38	0.012
M2	61	0.013
NGC 6397	15	0.012
M15	41	0.015

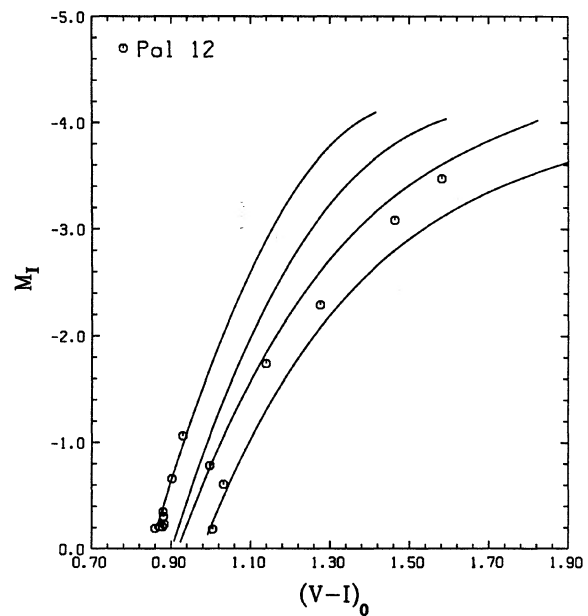


FIG. 11. Individual giants in the cluster Pal 12 shown in the $(M_I, (V-I)_0)$ plane together with the giant branch loci for the clusters M15, M2, NGC 1851, and 47 Tuc. A distance modulus $(m-M)_V = 16.46$ and a reddening $E(B-V) = 0.02$ mag have been used to place the Pal 12 points in this plot.

relative separation of the NGC 1851 and 47 Tuc giant branches at the M_I magnitude of the star. The Pal 12 abundance that results from this method is $[\text{Fe}/\text{H}] = -1.09 \pm 0.06$ dex, where the error reflects only the dispersion in the individual values determined. It is of some interest to note that the Pal 12 apparent visual distance modulus also resulting from this process (16.46) agrees well with that (16.42) given by Stetson *et al.* (1989) from isochrone fits. We further note that if we replace the NGC 1851 giant branch with that of NGC 362 (cf. the discussion above), the resulting Pal 12 abundance estimate is, at $[\text{Fe}/\text{H}] = -1.00 \pm 0.08$ dex based on the four brightest giants only, not significantly altered.

Alternatively, we can use the red horizontal branch stars present in the c - m diagrams of NGC 1851, Pal 12, and 47 Tuc to make an estimate of the abundance of Pal 12 that is independent of the LDZ scale: we simply superpose the red HB stars in all three clusters, after correcting for reddening differences, and then evaluate the locations of the Pal 12 giants relative to the NGC 1851 and 47 Tuc giant branches as before. The results of this process are shown in Fig. 12. Here the NGC 1851 data from Fig. 4 have been shifted by $\delta I = 0.818$ mag and $\delta(V - I) = 0.00$ mag (there being no reddening difference), while the equivalent shifts for 47 Tuc are 3.045 and -0.027 mag, respectively. The Pal 12 abundance that is then deduced is $[\text{Fe}/\text{H}] = -1.04 \pm 0.05$ dex, in excellent agreement with the first estimate. Again the error reflects only the error in the individual determinations. The agreement between the two methods also indicates that the LDZ distance scale is not grossly in error.

We thus adopt as our best estimate of the abundance of Pal

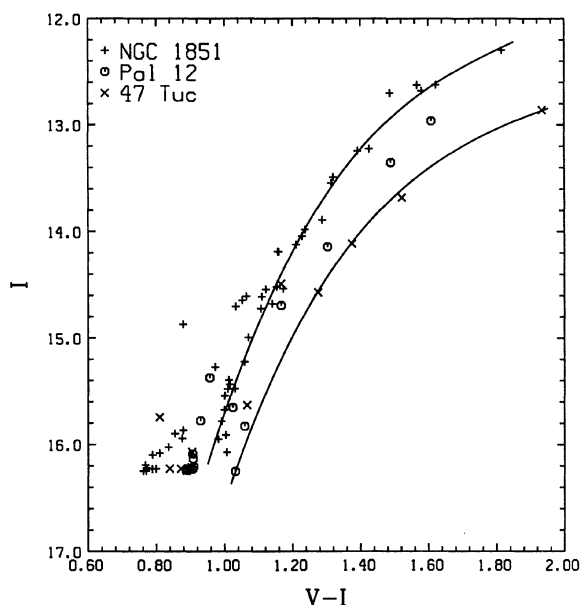


FIG. 12. Individual giants in the cluster Pal 12 (open symbols) shown in the $(I, V - I)$ plane. Also shown are individual stars and giant branch loci for the clusters NGC 1851 (plus symbols) and 47 Tuc (\times symbols). The NGC 1851 and 47 Tuc points have been placed in this diagram by shifting in $V - I$ to compensate for reddening differences and altering the I magnitudes to force the mean red horizontal branch magnitudes of these clusters to agree with that of Pal 12.

12 the value $[\text{Fe}/\text{H}] = -1.06 \pm 0.12$ dex, where the error estimate now allows for the uncertainties in the reddenings (± 0.02 mag) and in the abundances of the calibrating clusters (± 0.07 dex) as well as the dispersion from the individual measurements. This abundance is very similar to that quoted previously for this cluster [see Stetson *et al.* (1989) for an exhaustive discussion]. It lies close to the maximum observed for halo clusters (Da Costa and Seitzer 1989), though this is perhaps not surprising given that Pal 12 is the youngest halo cluster for which a reliable age estimate has been derived (Stetson *et al.* 1989).

The location of the Eridanus stars in the $(M_I, (V - I)_0)$ plane is shown in Fig. 13 together with the giant branches for M15, NGC 6752, NGC 1851, and 47 Tuc. We have used the same iterative technique described above to place the Eridanus stars in this diagram, assuming $E(B - V) = 0.03$ for the cluster reddening and $V = 20.24$ for the apparent magnitude of the horizontal branch (Da Costa 1985). The abundance was then determined from the location of the seven brightest giants in this diagram (excluding the probable field star 12) relative to the NGC 6752 and NGC 1851 giant branches, again in the same way as discussed above for Pal 12. The resulting abundance estimate for the Eridanus cluster is $[\text{Fe}/\text{H}] = -1.50 \pm 0.15$ dex, where the uncertainty includes the contributions from the uncertainties in the reddening and in the calibrating cluster abundances as well as the small (± 0.02 dex) scatter from the individual stars. This abundance compares favorably with that (-1.35 ± 0.2 dex) determined from the $(B - V)_{0,g}$ value for this cluster by Da Costa (1985). Thus the Eridanus cluster retains its distinction as one of the most metal-rich clusters in the extreme outer Galactic halo.

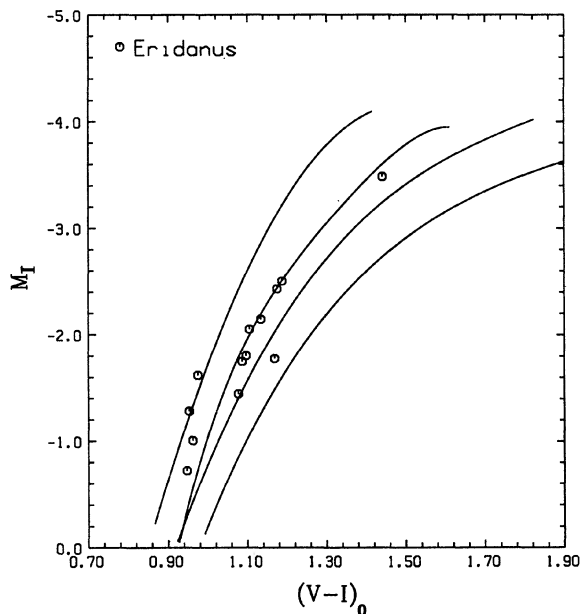


FIG. 13. Individual giants in the Eridanus cluster shown in the $(M_I, (V - I)_0)$ plane together with the giant branch loci for the clusters M15, NGC 6752, NGC 1851, and 47 Tuc. A distance modulus $(m - M)_V = 19.68$ and a reddening $E(B - V) = 0.03$ mag have been used to place the Eridanus points in this plot.

IV. COMPARISON WITH THEORY

Since the LDZ distance scale adopted here has as its basis theoretical models of horizontal branch stars, it is important to check its validity in as many ways as practical. One way of doing this is to compare our globular cluster observations, interpreted using the LDZ scale, with the predictions of other areas of stellar evolution theory to see if consistency can be found. We shall explore this question in this section by first comparing our results with theoretical predictions of the luminosity of the helium core flash, and then by investigating the extent to which our observations agree with the giant branch data available in the Revised Yale Isochrones (Green, Demarque, and King 1987; hereafter referred to as RYI).

a) Bolometric Corrections

A comparison between theory and observation for the luminosity of the helium core flash is best made using bolometric magnitudes, for the following reasons. First, bolometric magnitudes, or more correctly luminosities in terms of L_{sun} , are the direct output of the theory calculations. Conversion of the theoretical luminosities to any other quantity, such as M_V , automatically introduces uncertainty, particularly as such conversions generally involve the temperature of the stellar model, which, given its sensitivity to convective theories and adopted boundary conditions, is a much less well determined quantity. Second, on the observational side, the extensive IR photometry of Frogel, Persson, and Cohen (1983, and references therein) (hereafter referred to as FPC) yields bolometric magnitudes for many globular cluster red giants. These bolometric magnitudes were *empirically determined* for the most part by directly integrating the flux from the star via the observed *UBVJHK* photometry. Assumption of a distance scale then gives M_{bol} values.

However, in order to make use of our own observations, we need to generate a relation which will allow us to convert our M_I values, on the LDZ distance scale, to M_{bol} values, also on the LDZ distance scale. To do this we have adopted the following procedure. For those stars common either to our observations and FPC, or to the V, I photometry of Lloyd Evans (1983) and FPC, we have computed the difference (i.e., the bolometric correction to the I magnitude, BC_I) between M_I and M_{bol} , using the LDZ scale; the tabulated FPC M_{bol} values being adjusted appropriately to allow for FPC's use of a different distance scale. These bolometric corrections to the I magnitude are shown as a function of $(V-I)_0$ in Fig. 14. A least-squares fit to these data yields the relation

$$BC_I = 0.881 - 0.243(V-I)_0. \quad (2)$$

The dispersion about this fitted relation is only 0.057 mag and is entirely consistent with the observational errors inherent in the individual BC_I values. Further, there is no indication of any metal abundance sensitivity. This relation is essentially identical to that given in Mould, Kristian, and Da Costa (1984), which is not surprising since both relations were determined in the same way and since the bolometric correction itself is independent of the assumed distance scale. With this relation we can now calculate M_{bol} values from our V, I photometry.

b) $M_{\text{bol}}(Ist)$: Observations versus Theory

In Fig. 15 we plot against abundance the bolometric magnitude, determined using Eq. (2) and the LDZ distance scale, of the brightest reddest giant branch star in our photometry sample for each of the six clusters studied. Also plotted are equivalent data for NGC 362 and M5 using the photometry of Lloyd Evans (1983). The individual points

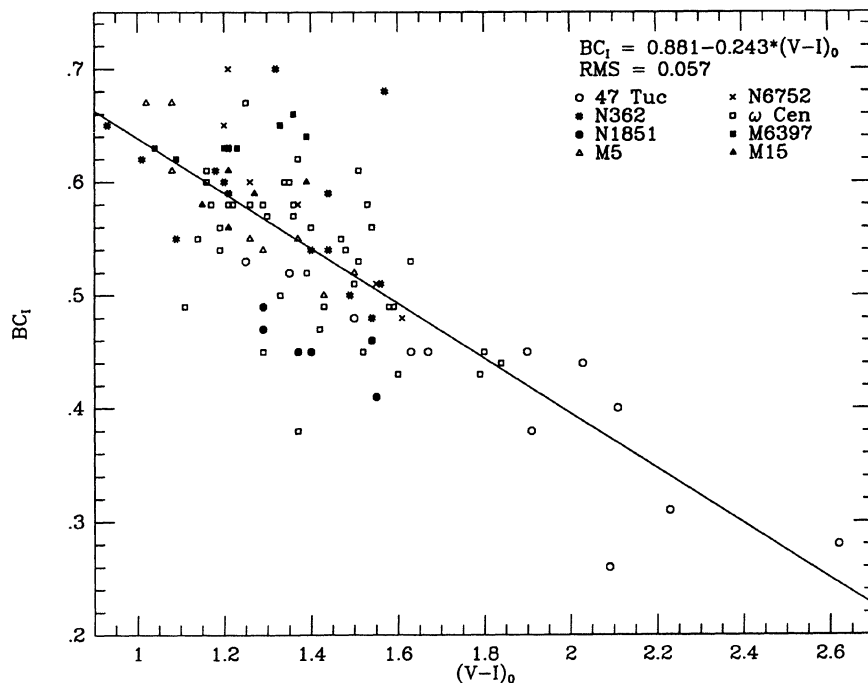


FIG. 14. Bolometric correction to the I magnitude, BC_I , plotted against $(V-I)_0$ color for those stars having both an empirical bolometric magnitude determined by Frogel, Persson, and Cohen (1983, and references therein) and V, I photometry from either Lloyd Evans (1983) or this paper. The solid line is a least-squares fit to these data points.

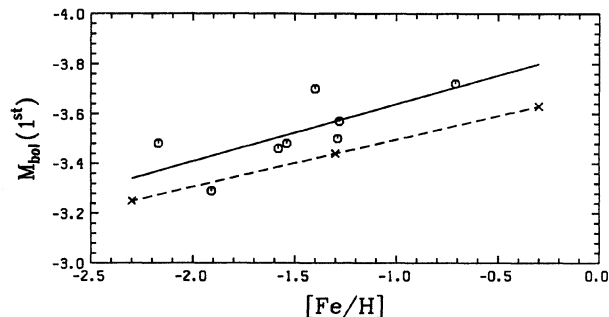


FIG. 15. Comparison of the bolometric magnitude of the brightest giant in each of the eight clusters (M15, NGC 6397, M2, NGC 6752, M5, NGC 362, NGC 1851, and 47 Tuc) with the predictions of stellar evolution theory as a function of abundance. The open symbols are the individual cluster points and the solid line is the least-squares fit to these data. The LDZ distance scale has been used in deriving the cluster $M_{\text{bol}}(1\text{st})$ values. The \times symbols represent the theoretical value for the luminosity of the helium core flash for $Y = 0.23$ and an age of 15 Gyr at Z values of 0.0001, 0.001, and 0.01, respectively. These points have been interpolated from the Sweigart and Gross (1978) giant branch tracks via the Revised Yale Isochrones. The three individual theory points are joined by a dashed line. Note the relatively good agreement, particularly with respect to the slope of the relations, between theory and observation.

are given in Table XII. Some comments on these choices are appropriate here, particularly with regard to how our choice of the “brightest star” compares with similar ones made in Frogel, Cohen, and Persson (1983) (hereafter referred to as FCP).

For 47 Tuc, as noted above, the brightest and reddest giants are all variables. Consequently, the assigning of stars to the AGB or the red giant branch is not straightforward. Frogel, Persson, and Cohen (1981) give reasons for assigning the large-amplitude (at least in B) long-period variables V1–V4 to the AGB. We concur with their discussion and suggest that by this criterion, V8 should also be considered an AGB star. On the other hand, Frogel, Persson, and Cohen (1981) also argue that the less luminous, smaller amplitude shorter period stars should contain at least some red giant branch stars. For this reason, we decided to average the bolometric magnitudes for the three most luminous variables with multiple observations in Lloyd Evans (1983). These stars are V11, Lee (1977) 1421, and V28; their bolometric magnitudes are -3.85 , -3.70 , and -3.62 , respec-

tively, resulting in a $M_{\text{bol}}(1\text{st})$ value of -3.72 for this cluster. FCP give $M_{\text{bol}}(1\text{st})$ for 47 Tuc as -3.85 (on the LDZ scale), based on a single IR observation of star V8 (which we consider an AGB star), while, again on the LDZ scale, their data give $M_{\text{bol}} = -3.83$ for V11, also from a single IR observation. Thus it is conceivable that our estimate of $M_{\text{bol}}(1\text{st})$ for this cluster is too faint by 0.1–0.15 mag, but this will not have any major consequences for the discussion below. FCP also note that the search for bright red stars in this cluster is essentially complete.

For NGC 1851, we give the M_{bol} value of -3.50 for the star DA6, which is the brightest and reddest star in the NGC 1851 c–m diagram in Fig. 4. FCP list $M_{\text{bol}}(1\text{st})$ as -3.66 (on the LDZ scale) based on an unidentified star in the cluster center found by IR scanning. Given the possibility of background contamination in this concentrated cluster, we prefer our value but again note that it should perhaps be regarded as a lower limit on the true value of $M_{\text{bol}}(1\text{st})$ for this cluster.

In NGC 362, NGC 6752, NGC 6397, and M15 the brightest reddest star in our sample is the same as that chosen by FCP, who note the possibility that in all four of these clusters, brighter giants may exist closer to the cluster center. For M2, however, which was not studied by FCP, this is not likely to be the case since our M2 sample includes stars measured on frames of the center of this cluster. Finally we note that for M5, the star we have chosen to define $M_{\text{bol}}(1\text{st})$ is some 0.3 mag brighter than the star used by FCP on the LDZ distance scale, a result consistent with the comments for this cluster in Table 29 of FCP. In this context it is perhaps also worth noting that the Monte Carlo simulations of Crocker and Rood (1984) (cf. FCP) indicate that the probability of observing a cluster giant within 0.1 mag of the actual giant branch tip is quite large, even for relatively small samples of giants.

Also shown in Fig. 15 is the theoretical prediction for the luminosity of the helium core flash based on the giant branch models of Sweigart and Gross (1978). The theory line is appropriate for a helium abundance $Y = 0.23$, the same as that adopted in our use of the LDZ distance scale. This relation has been derived by interpolating between the RYI for $Y = 0.2$ and $Y = 0.3$ at an assumed age of 15 Gyr. The interpolation was done only at abundances of $Z = 0.0001$, 0.001, and 0.01, which are the abundances at which the Sweigart and Gross (1978) giant branch calculations were made, to minimize possible systematic uncertainties. The output L/L_{sun} values were converted to M_{bol} values by assuming $M_{\text{bol}}(\text{sun}) = 4.79$. The use of an age of 15 Gyr is not crucial, since changes in the age (or ages) assumed of the order of 2–3 Gyr alter the theoretical helium core flash luminosities by only ~ 0.02 mag or less at constant abundance.

There are a number of conclusions to be drawn from Fig. 15 and we now address them in turn. First, considering the observational points alone, an unweighted least-squares fit yields the relation $M_{\text{bol}}(1\text{st}) = -0.23[\text{Fe}/\text{H}] - 3.87$, with a rms deviation about the fitted line of 0.09 mag. This dispersion is completely consistent with that expected from the uncertainties in the $M_{\text{bol}}(1\text{st})$ values and the expected statistical sampling error (cf. Crocker and Rood 1984; FCP). Such a small dispersion in fact supports the conclusion, first drawn by FCP, that at fixed abundance, there is very little intrinsic dispersion in the absolute magnitude of the horizontal branch in globular clusters.

Second, comparing now the observations with the theo-

TABLE XII. Brightest cluster giants.

Cluster	Star	$M_{\text{bol}}(1\text{st})$	Note
47 Tuc	see note 1	-3.72	1
NGC 1851	DA6	-3.50	2
NGC 6752	A31	-3.48	
M2	$-46 + 60$	-3.46	
NGC 6397	RGO469	-3.29	
M15	I-12	-3.48	
NGC 362	V2	-3.57	3
M5	TLE 1	-3.70	3

Notes to TABLE XII

- (1) M_{bol} given is mean of M_{bol} values for stars V11, Lee 1421, and V28.
- (2) FCP suggest stars up to 0.15 mag brighter may exist in cluster center.
- (3) V, I photometry from Lloyd Evans (1983).

retical prediction line, it is apparent that they are in relatively satisfactory agreement. This is particularly true for the slope of the theory relation, which, at -0.19 mag/dex, is identical to within the uncertainties with the slope (-0.23 ± 0.09 mag/dex) of the least-squares fit. There is, however, an offset of approximately 0.12 mag between the theory and the observed points, with the observations, on the LDZ distance scale, being brighter. Because the LDZ distance scale is based on theoretical calculations of horizontal branch stars, this offset is truly a measure of the degree of consistency between the calculations of giant branch and horizontal branch evolution. The size of the offset is encouragingly small and may only reflect the breakdown of one or more of the assumptions made in modeling complex physical processes. Alternatively, it may be a consequence of our lack of detailed knowledge of the hydrodynamic phenomena that occur at the helium flash. Certainly, the offset would be resolved if the core masses of zero-age horizontal branch stars are slightly smaller than the core mass at the helium flash, or equivalently, if the luminosity of the helium flash for a given core mass on the giant branch is slightly increased. However, it is beyond the scope of this paper to discuss these possibilities further.

On the other hand we regard the equation

$$M_{\text{bol}}(1\text{st}) = -0.19[\text{Fe}/\text{H}] - 3.81, \quad (3)$$

in which we have adopted the theoretical slope but determined the intercept from the observations, as the most appropriate relation between abundance and the bolometric magnitude of the first giant branch tip for the LDZ distance scale. This relation, together with Eq. (2), can then be used with V, I observations either to determine distances to stellar populations known to be old, or to constrain the numbers of upper AGB stars (i.e., younger objects) in systems of known distance (cf. MKD).

Regardless of the origin of the offset in luminosity between theory and observation in Fig. 15, the agreement in slope has an important consequence. If we parameterize the distance scale by an equation of the form $M_V(\text{RR}) = a[\text{Fe}/\text{H}] + b$, then Fig. 15 supports the value of a (0.17) contained in the LDZ distance scale. This, in turn, has a number of implications, not the least of which is the occurrence of a significant age-abundance relation among the halo globular clusters (see LDZ for details). If we had adopted instead a different value of a , then the slope defined by the observed points in Fig. 15 would have been different. For example, using the distance scale of Sandage (1982), in which $M_V(\text{RR}) = 1.39 + 0.35[\text{Fe}/\text{H}]$, the least-squares fit to the (appropriately modified) observed points, shown in Fig. 16, has a slope (0.03 ± 0.09 mag/dex) that is different from the theoretical value by more than 2σ . Hence if the Sandage (1982) distance scale is ultimately judged correct, then it will have serious implications not only for theoretical calculations of the horizontal branch, but also, as is evident from Fig. 16, for similar calculations of red giant evolution.

Finally, Fig. 15 also allows us to make some comments on the recent paper by Vandenberg and Durrell (1990) (hereafter referred to as VD). In their paper VD propose use of the V magnitude of the giant branch tip as a relative distance indicator: after correcting for reddening differences, giant branch tips are aligned in V , allowing relative ages to be inferred from the resulting relative locations of cluster turn-offs. VD go on to use this procedure to argue that there is no detectable difference in age between the clusters NGC 288,

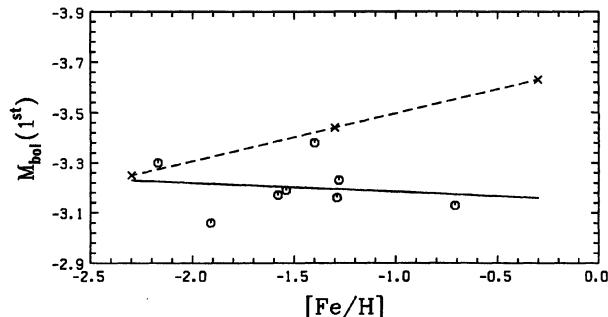


FIG. 16. As for Fig. 15, except that the Sandage distance scale, which has steeper dependence of $M_V(\text{RR})$ on $[\text{Fe}/\text{H}]$ than the LDZ scale, has been used to calculate the cluster $M_{\text{bol}}(1\text{st})$ values. The solid line is again the least-squares fit to the observed points. The theory points are unaltered from Fig. 15. Note the significant disagreement in slope between theory and observation as compared to Fig. 15.

NGC 362, and M5. This contradicts the findings of others (e.g., Demarque *et al.* 1989; Bolte 1989; Green and Norris 1990) that NGC 288 is some 2–5 Gyr older than NGC 362. The small dispersion in Fig. 15 indicates that VD's technique, when applied to clusters of similar abundance, should yield quite precise relative distances (cf. Crocker and Rood 1984; FCP) and therefore accurate relative ages, *provided the tip of the giant branch is correctly identified*.

As regards the relative ages of NGC 288 and NGC 362 inferred by VD, this latter point proves to be the crucial one. VD (see footnote 2 of their paper) choose to ignore the NGC 288 star V1 (Alcaino 1975, star A260) and set the NGC 288 giant branch tip some 0.2 mag fainter at $V = 12.70$, essentially at the V magnitude of the next brightest giant, A96. Both these stars have V, I photometry from Lloyd Evans (1983) and we can follow the same process as was done above to calculate their bolometric magnitudes. Adopting $E(B - V) = 0.04$, $V(\text{HB}) = 15.3$, and $[\text{Fe}/\text{H}] = -1.4$ dex, all from Armandroff (1989), the LDZ distance scale, and the bolometric corrections of Eq. (2), the Lloyd Evans (1983) photometry then yields $M_{\text{bol}} = -3.50$ for V1 and $M_{\text{bol}} = -2.81$ for A96. FPC list, after correction to the LDZ distance scale, very similar values of -3.55 and -2.91 , respectively, from their IR photometry. Comparison with Fig. 15 then indicates that the star V1 has the correct bolometric magnitude to be identified with the NGC 288 giant branch tip, while star A96 is clearly much too faint. Thus, unless the absolute magnitude of the horizontal branch of NGC 288 differs drastically from that in other clusters of similar abundance, which based on the discussion above we consider extremely unlikely (see also FCP), we suggest that VD have erred in their choice of the V magnitude of the NGC 288 giant branch tip; a more appropriate value is some 0.2 mag or so brighter. Use of such a value will result in a NGC 362 turnoff that is brighter than that of NGC 288 by this amount [cf. Fig. 2(a) of VD with $\Delta V = -0.05$ rather than $+0.15$], thus supporting, rather than contradicting, an age difference between these clusters of some 2–3 Gyr as advocated by Bolte (1989) and Green and Norris (1990). Hence the giant branch tip luminosities of these clusters, as interpreted here, support the assertion that age is an important parameter governing the horizontal branch morphology of Galactic globular clusters.

c) Theoretical Giant Branches

In Fig. 17 we plot the observed giant branch curves for the clusters M15, M2, NGC 6752, NGC 1851, and 47 Tuc together with four theoretical giant branches calculated from the RYI data. These theoretical giant branches are for a helium abundance $Y = 0.23$ and metal abundances $Z = 0.0001, 0.0006, 0.001,$ and 0.004 . The corresponding $[\text{Fe}/\text{H}]$ values are $-2.3, -1.52, -1.3,$ and -0.7 dex, respectively. Ages of 15 Gyr have been assumed for the two more metal-poor giant branches, while for the more metal-rich pair, the age assumed is 13 Gyr. None of the discussion in this section is affected by these particular age choices.

Given the cluster abundances listed in Table IX, one would expect, perhaps naively, that there would be a reasonably close correspondence between the theoretical and the observed giant branches. That is quite evidently not the case in Fig. 17, where the theoretical giant branches are generally too faint and/or too red compared to the observations. Since the theory and the observations were in much better accord as regards M_{bol} (1st) and the giant branch tip, one is led to suspect the color-temperature and bolometric correction procedures inherent in the RYI as the major source of the discrepancy.

The color-temperature and bolometric corrections in the RYI are "semiempirical" [see Green (1988) for a discussion], as distinct from those based strictly on model atmosphere calculations (e.g., Vandenberg and Bell 1985). In

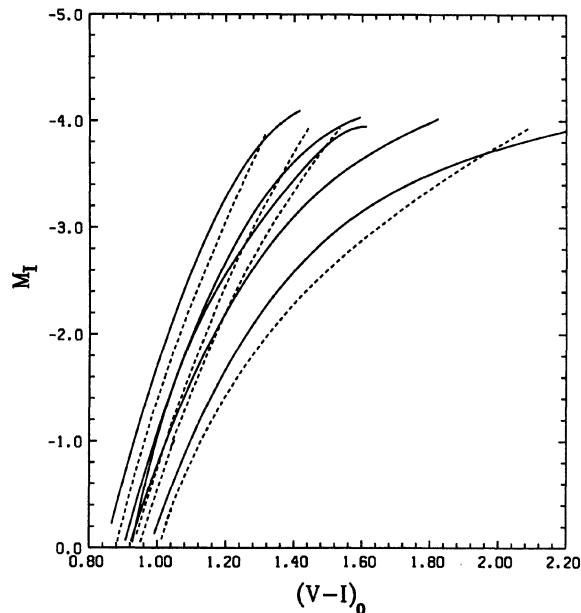


FIG. 17. Comparison of the observed giant branches for M15, M2, NGC 6752, NGC 1851, and 47 Tuc (solid curves) with the giant branches for $Y = 0.23$ and Z values of $0.0001, 0.0006, 0.001,$ and 0.004 , respectively, from the Revised Yale Isochrones (dashed curves) in the $(M_I, (V-I)_0)$ plane. The cluster giant branch absolute magnitudes are on the LDZ distance scale. Note that the 47 Tuc observed giant branch continues to $(V-I)_0$ colors of approximately 2.6, but this is not shown in order to improve the clarity of the figure.

particular, the globular cluster giant branch data and the $V-K$ temperature scale contained in FPC and FCP were used in the RYI, for a selected set of clusters, to correct the temperatures of the original Sweigart and Gross (1978) giant branch tracks. This correction was required because the models were calculated with a mixing length parameter $\alpha = 1.0$ instead of the now more generally accepted value of $\alpha = 1.5$ to 1.6 , yielding effective temperatures that were clearly too cool [see the discussion following Green (1988)]. $UBVRI$ photometry of giants in these same clusters then defined the temperature-to-color conversion. Although not explicitly noted by Green (1988), this temperature correction process, in which a temperature on a Sweigart and Gross (1978) track for a particular Z is mapped at constant luminosity to a new temperature given by the FCP data for the corresponding $[\text{Fe}/\text{H}]$, necessarily depends on the distances assumed for the calibrating clusters. The distance scale adopted (Green 1989) was that of FPC, in which $M_V(\text{HB}) = +0.6$ for $[\text{Fe}/\text{H}] < -1.0$, $M_V(\text{HB}) = +0.7$ for $-1.0 < [\text{Fe}/\text{H}] < -0.8$, and $M_V(\text{HB}) = +0.8$ for $[\text{Fe}/\text{H}] > -0.8$ dex. Since this is different from the LDZ scale adopted here, it is not surprising then that the theoretical giant branches do not fit our observations.

It is worth emphasizing this point once again: the temperature-color conversion process and, to a lesser extent, the bolometric corrections (because they are a function of color/temperature) inherent in the RYI giant branches are appropriate only for the FPC distance scale. Therefore, the RYI giant branches are strictly not applicable at any other chosen distance. This fact negates to a large extent their use [cf. Green (1988) footnote, p. 91] to help define the distance modulus of a cluster by requiring a good fit between the RYI and the observations over the entire c-m diagram. Only if the resulting modulus is near that implied by the FPC scale will the giant branch fit be valid. In this context we should also emphasize that the main sequence and subgiant branch calibration in the RYI was carried out in an entirely different fashion (Green 1988). Consequently, main sequence and subgiant branch fits with the RYI are not constrained to a particular distance scale.

We show in Fig. 18 the same observational and theoretical giant branches as in Fig. 17, except that now the observations are on the FPC distance scale. Not surprisingly, given the discussion above, the agreement is much improved. The agreement for 47 Tuc for $M_I > -3.0$ is particularly good, though this is not unexpected since 47 Tuc was one of the clusters involved in the calibrating process (Green 1988). Similarly, the agreement for the more metal-poor clusters is relatively satisfactory for $M_I > -3.0$. There is a general tendency for the theoretical giant branches to lie $0.01-0.03$ mag redder than the observations, but such differences are within the uncertainties in the theoretical temperature-color conversion, the assumed cluster reddenings and $V(\text{HB})$ values, and the observed $V-I$ colors themselves. More disturbing is the apparent difference between the theoretical and observed giant branches at the brightest magnitudes. There is a definite systematic trend in that the observed giant branches become progressively redder than those of the theory as the giant branch tip is approached, with the difference increasing with increasing abundance. This difference should be kept in mind when observations are interpreted on the basis of the RYI giant branches alone (cf. Freedman 1989). It probably results from the procedures adopted in shifting the

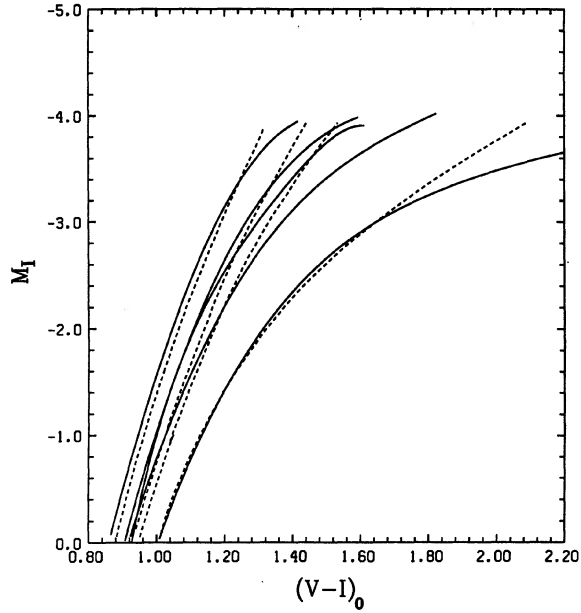


FIG. 18. As for Fig. 17, except that now the cluster giant branches are plotted at absolute magnitudes that correspond to the distance scale adopted by Frogel, Persson, and Cohen (1983). This particular distance scale is implicitly built into the Revised Yale Isochrone giant branches. Note once more that the 47 Tuc observed giant branch continues to $(V-I)_0$ colors of approximately 2.6, but this is not shown in order to improve the appearance of the figure.

Sweigart–Gross giant branches in effective temperature (Green 1989), but in any case one must question the validity of the model assumptions (e.g., convective theory and/or atmospheric boundary conditions) at the lowest temperatures and gravities. Interestingly, the calculations of VandenBerg (1984) do not seem [at least in the $(M_{\text{bol}}, \log T_{\text{eff}})$ plane] to show as large an effect, but without the availability of these latter calculations in the $(M_I, V-I)$ plane, the question cannot be pursued further.

We conclude, therefore, that once the assumptions inherent in the RYI giant branches are correctly allowed for, the agreement between theory and observation is satisfactory for all but the brightest giants. These appear to be redder than predicted by the RYI, with the size of the offset increasing with increasing abundance.

V. SUMMARY

In this paper we have presented CCD photometry in the V, I (Cousins) bandpasses for a large number of giants in eight galactic globular clusters. Based on both internal checks and external comparisons with globular cluster stars measured with conventional photoelectric photometry, we believe that our CCD photometry is accurately on the standard system and that the individual random photometric errors do not exceed 0.02 mag. We have used this photometry, together with the assumption of the LDZ distance scale, in which $M_V(\text{RR}) = 0.82 + 0.17[\text{Fe}/\text{H}]$, to derive the following results.

(1) The $(V-I)_0$ color of the giant branch accurately ranks clusters in metal abundance and thus it can be used to

determine metal abundances and metal abundance dispersions in old stellar populations. Based on the LDZ distance scale and abundances for the calibrating clusters from Armandroff (1989), we derived the following relation between giant branch color and abundance:

$$[\text{Fe}/\text{H}] = -15.16 + 17.0(V-I)_{0,-3} - 4.9[(V-I)_{0,-3}]^2,$$

where $(V-I)_{0,-3}$ is the color of the giant branch at an absolute magnitude $M_I = -3.0$. The relation is valid for $-2.2 < [\text{Fe}/\text{H}] < -0.7$ dex.

(2) For the six standard clusters, the observed color dispersions about the fitted giant branch curves are very small (0.02 mag or less) and consistent with the photometric errors alone. Thus there is no evidence for any intrinsic giant branch color width in these clusters, or equivalently no indication of any intrinsic spread in the abundances of the elements that control the giant branch effective temperatures. We set 3σ upper limits on any such abundance spread in the range 0.04–0.09 dex.

(3) Using CCD photometry of their giants obtained in the same way as for the calibrating clusters, we derive abundances of $[\text{Fe}/\text{H}] = -1.06 \pm 0.12$ and -1.50 ± 0.15 dex, respectively, for the globular clusters Pal 12 and Eridanus. These values are consistent with earlier less precise estimates for these clusters.

(4) Based on the IR photometry of FPC, the V, I photometry of Lloyd Evans (1983), and our own data, we derived a relation that yields the bolometric correction to the I magnitude for red giants as a function of $(V-I)_0$ color. This relation is given by Eq. (2). With this relation, and the assumption of the LDZ distance scale, the bolometric magnitudes of the brightest red giants in the clusters were determined. These data were found to agree rather well with the predictions of stellar evolution theory for the luminosity of the helium core flash. In particular, the slope of the relation between $M_{\text{bol}}(1\text{st})$ and $[\text{Fe}/\text{H}]$ found observationally agreed to within the uncertainties with that predicted theoretically, though the observations are ~ 0.12 mag too bright compared to theory. The agreement in slope, however, supports the relation between $M_V(\text{RR})$ and $[\text{Fe}/\text{H}]$ contained in the LDZ distance scale. A similar plot, with the bolometric magnitudes determined with the distance scale of Sandage (1982), gives a much poorer agreement with theory. The calibration of $M_{\text{bol}}(1\text{st})$ with $[\text{Fe}/\text{H}]$ for the LDZ distance scale is given by Eq. (3). We have also used these data to argue that VandenBerg and Durrell (1990) have erred in their choice for the V magnitude of the NGC 288 giant branch tip, and that a more appropriate choice supports the existence of an age difference between this cluster and NGC 362, as recently suggested by others.

(5) The observed giant branches were also compared with those contained in the Revised Yale Isochrones. This led to the realization that the “semiempirical” method used to generate the RYI giant branches from the Sweigart and Gross (1978) giant branch models requires a particular distance scale, that of FPC, to be followed for the comparison to be valid. When this adjustment is made to the observations, the agreement is acceptable. However, at the highest luminosities and lowest temperatures, the observations deviate substantially from the RYI giant branches, becoming increasingly redder as the giant branch tip is reached. Further, the size of this discrepancy increases with increasing metal abundance.

One of us (GDaC) would like to express his thanks to the Visitor Support Staff at CTIO for their assistance in making the observing runs a success. We are also grateful to Drs.

Pierre Demarque, Elizabeth Green, John Norris, Marc Pinsonneault, and Robert Zinn for interesting discussions concerning the content of this paper.

REFERENCES

- Alcaino, G. (1972). *Astron. Astrophys.* **16**, 220.
 Alcaino, G. (1975). *Astron. Astrophys. Suppl.* **21**, 15.
 Alcaino, G. (1977). *Astron. Astrophys. Suppl.* **29**, 397.
 Armandroff, T. E. (1988). *Astron. J.* **96**, 588.
 Armandroff, T. E. (1989). *Astron. J.* **97**, 375.
 Armandroff, T. E., and Zinn, R. (1988). *Astron. J.* **96**, 92.
 Arp, H. C. (1955). *Astron. J.* **60**, 317.
 Auriere, M., and Cordoni, J.-P. (1983). *Astron. Astrophys. Suppl.* **51**, 135.
 Bolte, M. (1989). *Astron. J.* **97**, 1688.
 Buonanno, R., Buscema, G., Corsi, C. E., Iannicola, G., and Fusi Pecci, F. (1983). *Astron. Astrophys. Suppl.* **51**, 83.
 Cannon, R. D. (1974). *Mon. Not. R. Astron. Soc.* **167**, 551.
 Cannon, R. D., and Stobie, R. S. (1973). *Mon. Not. R. Astron. Soc.* **162**, 227.
 Cousins, A. W. J. (1976a). *Mem. R. Astron. Soc.* **81**, 25.
 Cousins, A. W. J. (1976b). *Mon. Not. Astron. Soc. S. Afr.* **35**, 70.
 Cousins, A. W. J. (1984). *S. Afr. Astron. Obs. Circ.* **8**, 59.
 Crocker, D. A., and Rood, R. T. (1984). In *Observational Tests of Stellar Evolution Theory*, IAU Symposium No. 105, edited by A. Maeder and A. Renzini (Reidel, Dordrecht), p. 159.
 Da Costa, G. S. (1982). *Publ. Astron. Soc. Pac.* **94**, 769.
 Da Costa, G. S. (1985). *Astrophys. J.* **291**, 230.
 Da Costa, G. S. (1990). In *CCDs in Astronomy*, Astronomical Society of the Pacific Conference Series, edited by G. Jacoby (Astronomical Society of the Pacific, San Francisco) (in press).
 Da Costa, G. S., and Seitzer, P. (1989). *Astron. J.* **97**, 405.
 Dean, J. F., Warren, P. R., and Cousins, A. W. J. (1978). *Mon. Not. R. Astron. Soc.* **183**, 569.
 Demarque, P., Lee, Y.-W., Zinn, R., and Green, E. M. (1989). In *The Abundance Spread within Globular Clusters: Spectroscopy of Individual Stars*, edited by G. Cayrel de Strobel, M. Spite, and T. Lloyd Evans (Paris Observatory, Paris), p. 97.
 Demers, S. (1969). *Astron. J.* **74**, 925.
 Freedman, W. L. (1989). *Astron. J.* **98**, 1285.
 Frogel, J. A., Cohen, J. G., and Persson, S. E. (1983). *Astrophys. J.* **275**, 773 (FCP).
 Frogel, J. A., Persson, S. E., and Cohen, J. G. (1981). *Astrophys. J.* **246**, 842.
 Frogel, J. A., Persson, S. E., and Cohen, J. G. (1983). *Astrophys. J. Suppl.* **53**, 713 (FPC).
 Graham, J. A. (1982). *Publ. Astron. Soc. Pac.* **94**, 244.
 Green, E. M. (1987). Private communication.
 Green, E. M. (1988). In *Calibration of Stellar Ages*, edited by A. G. D. Philip (Davis, Schenectady), p. 81.
 Green, E. M. (1989). Private communication.
 Green, E. M., Demarque, P., and King, C. R. (1987). *The Revised Yale Isochrones and Luminosity Functions* (Yale University Observatory, New Haven) (RYI).
 Green, E. M., and Norris, J. (1990). *Astrophys. J. Lett.* **353**, L17.
 Harris, W. E. (1975). *Astrophys. J. Suppl.* **29**, 397.
 Harris, W. E., and Canerna, R. (1980). *Astrophys. J.* **239**, 815.
 Heasley, J. N., Christian, C. A., Friel, E. D., and Janes, K. A. (1988). *Astron. J.* **96**, 1312.
 Hesser, J. E., Harris, W. E., Vandenberg, D. A., Allwright, J. W. B., Shott, P., and Stetson, P. B. (1987). *Publ. Astron. Soc. Pac.* **99**, 739.
 Kustner, F. (1921). *Veröff. Sternw. Bonn* No. 15.
 Landolt, A. U. (1983). *Astron. J.* **88**, 439.
 Larson, R. B. (1988). In *Globular Cluster Systems in Galaxies*, IAU Symposium No. 126, edited by J. E. Grindlay and A. G. D. Philip (Kluwer, Dordrecht), p. 311.
 Lee, S.-W. (1977). *Astron. Astrophys. Suppl.* **27**, 381.
 Lee, Y.-W., Demarque, P., and Zinn, R. (1987). In *The Second Conference on Faint Blue Stars*, IAU Colloquium No. 95, edited by A. G. D. Philip, D. S. Hayes, and J. W. Liebert (Davis, Schenectady), p. 137.
 Lee, Y.-W., Demarque, P., and Zinn, R. (1990). *Astrophys. J.* **350**, 155 (LDZ).
 Lloyd Evans, T. (1983). *S. Afr. Astron. Obs. Circ.* **7**, 86.
 Mould, J., Kristian, J., and Da Costa, G. S. (1983). *Astrophys. J.* **270**, 471 (MKD).
 Mould, J., Kristian, J., and Da Costa, G. S. (1984). *Astrophys. J.* **278**, 575.
 Norris, J., Bessell, M. S., and Pickles, A. J. (1985). *Astrophys. J. Suppl.* **58**, 463.
 Pryor, C., McClure, R. D., Fletcher, J. M., Hartwick, F. D. A., and Kormendy, J. (1986). *Astron. J.* **91**, 546.
 Richer, H. B., Crabtree, D. R., and Pritchett, C. J. (1984). *Astrophys. J.* **287**, 138.
 Richer, H. B., and Fahlman, G. G. (1987). *Astrophys. J.* **316**, 189.
 Sandage, A. (1970). *Astrophys. J.* **162**, 841.
 Sandage, A. (1982). *Astrophys. J.* **252**, 553.
 Schoening, W. (1988). *Operation of the CCD Direct Imaging Camera for the #1 0.9-m Telescope* (NOAO/KPNO, Tucson).
 Stetson, P. B. (1981). *Astron. J.* **86**, 687.
 Stetson, P. B., Vandenberg, D. A., Bolte, M., Hesser, J. E., and Smith, G. H. (1989). *Astron. J.* **97**, 1360.
 Sweigart, A. V., and Gross, P. G. (1978). *Astrophys. J. Suppl.* **36**, 405.
 Vandenberg, D. A. (1984). In *Observational Tests of Stellar Evolution Theory*, IAU Symposium No. 105, edited by A. Maeder and A. Renzini (Reidel, Dordrecht), p. 143.
 Vandenberg, D. A., and Bell, R. A. (1985). *Astrophys. J. Suppl.* **58**, 561.
 Vandenberg, D. A., and Durrell, P. R. (1990). *Astron. J.* **99**, 221 (VD).
 Vidal, N. V., and Freeman, K. C. (1975). *Astrophys. J. Lett.* **200**, L9.
 Woolley, R. v. d. R., Alexander, J. B., Mather, L., and Epps, E. (1961). *R. Obs. Bull.* No. 43.
 Zinn, R. (1980). *Astrophys. J. Suppl.* **42**, 19.
 Zinn, R., and West, M. J. (1984). *Astrophys. J. Suppl.* **55**, 45.